1997

DNA-protamine interactions

Syamala Akkaraju
San Jose State University

DNA-PROTAMINE INTERACTIONS

A Thesis presented to

The Faculty of the Department of Chemistry

San Jose State University

In Partial Fulfillment of the

Requirements for the Degree

Master of Science

by

Syamala Akkaraju

May, 1997

APPROVED FOR THE DEPARTMENT OF CHEMISTRY

Pamela C Stacks

Dr. Pamela C. Stacks

Dr. Roger Biringer

Brenda Kesler

Dr. Brenda Kesler

M. Lou Lewandowski

APPROVED FOR THE UNIVERSITY

Abstract

DNA-Protamine Interactions

by Syamala Akkaraju

The objective of the research is to determine the dissociation rate constant and half life of the DNA-Protamine P2 complex using dynabeads as a solid support. Dynabeads are paramagnetic, uniform monodispersed polystyrene microspheres. Dynabeads substituted with P2 from hamster sperm were incubated with ^{33}P radiolabeled, 12 base pair DNA to form DNA-P2 complexes. The dissociation rate constant (k_2) complexes were determined using a dissociation protocol based on the dilution of the complexes. Quantitation of free DNA and bound DNA was determined by liquid scintillation counting after magnetic separation of complexes and free DNA.

The k_2 determined for P2-DNA complex is $6.7 \times 10^{-5} \pm 0.8 \times 10^{-5}$ s^{-1} at pH 7.4, 24 ^{0}C and 0.1 M [NaCl]. The effect of [NaCl] on k_2 was studied. As the concentration of NaCl was increased, the dissociation of the complexes increased, which suggests that electrostatic forces play an important role in the formation of DNA-P2 complexes.

Table Of Contents

List of Tables

List of Figures

List of Abbreviations

Reagents:

DNA	Deoxyribose nucleic acid
ATP	Adenosine-5'-triphosphate
HEPES	N-[2-hydroxyethyl]piperazine-N'-[2-ethanesulfonic acid]
TAPS	N-tris[Hydroxymethyl]methyl-3-amino-propanesulfonic acid)
DTT	Dithiothreitol
EDTA	Ethylenediaminetetraacetic acid

Amino acids:

A	alanine	M	methionine
C	cysteine	P	proline
F	phenylalanine	Q	glutamine
G	glycine	R	arginine
H	histidine	S	serine
I	isoleucine	T	threonine
K	lysine	V	valine
L	leucine	Y	tyrosine

INTRODUCTION

Protamines are the arginine rich proteins which cause the condensation of DNA in sperm cells. The long DNA molecules (about one meter long when fully extended in humans) have to be compacted in order to fit into cells which are few micrometers in diameter. Protamines cause about 10^6-fold condensation of the DNA molecules in sperm cells by the neutralization of the phosphodiester backbone of the DNA molecules. Histones are the basic proteins which mediate the compaction of the DNA in somatic cells. Protamines replace the histones during spermiogenesis. The DNA-protamine complex is insoluble (1), genetically inactive and biochemically inert (2). For these reasons the DNA repair mechanisms are disabled during the formation of the DNA-protamine complexes and any damages that occur in a sperm DNA are repaired only after fertilization (2).

There are two classes of mammalian protamines, protamine P1 and protamine P2. All the mammalian species examined have the genes for both P1 and P2. The gene for P1 is active in all the species of mammals, but the gene for P2 is active in only a few mammalian species. The sperm cells of bull, ram, rat, boar, guinea pig and rabbit contain only P1 while the sperm cells of human, hamster and mouse contain both P1 and P2. Two other protamines, P3 and P4, were isolated from human sperm. Since the primary amino acid sequence of P3 and P4 are similar to that of P2, they were classified under the superfamily P2. The protamines isolated from pisces and aves are different from those of

mammals. They vary in length and have more arginine residues. They do not have cysteine residues but contain proline unlike the mammalian protamine P1.

The primary amino acid sequence of P1 isolated from many mammalian species has been determined. The primary amino acid sequence of P1 isolated from bull, hamster, and human sperm are shown in Figure 1. All P1 molecules contain 50 amino acid residues and the primary amino acid sequence is highly conserved. About 50% of the total number of amino acids are arginines. Balhorn proposed dividing the P1 molecule into three structural domains (1), with the central polyarginine region flanked on both sides by smaller, relatively arginine deficient N and C-terminal domains. The central region consists of multiple DNA anchoring units that consist of three to seven arginines. These units are separated by one or more nonarginine amino acids. The smaller N and C-terminal domains consist of serine, threonine or tyrosine at specific locations. These are the possible phosphorylation sites. The N-terminal hexapeptide sequence is highly conserved as seen in Figure 1.

Balhorn et al. (3) studied the disulfide crosslinks in bull protamine P1 by titrating intact bull sperm with dithiothreitol (DTT) and following each modified cysteine residue with titrated iodoacetate. The results of these experiments showed that the N and C terminal ends of the bull protamine are folded inward towards the center of the molecule. The folds are locked in place by two intramolecular disulfide bridges as shown in Figure 2.

(ARYRCC)LTHSGSRCRRRRRRRCRRRRRRFGRRRRRRVCCRRYTVIRCTRQ

Bull protamine P1

(ARYRCC)RSKSRSRCRRRRRRCRRRRRRCCRRRRRRCCRRRRTYTLRCKRY

Hamster protamine P1

(ARYRCC)RSQSRSRYYRQRQRSRRRRRRSCQTRRRAMRCCRPRYRPRCRRH

Human protamine P1

Figure 1: The functional structure of mammalian P1 from bull, hamster and human proposed by Balhorn (1). The underscored regions represent the anchoring units which are the DNA binding sites. The six amino acids of the N-terminus shown in brackets comprise the protamine P1 specific hexapeptide, characteristic of the mammalian P1. All of them contain 50 amino acids and have 26, 29, 24 arginine residues respectively.

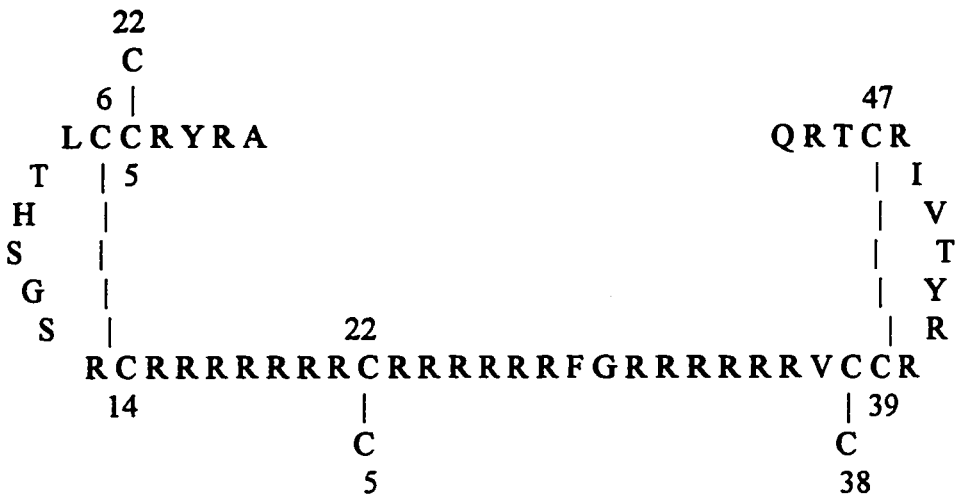

Figure 2: The two intramolecular and the three intermolecular disulfide linkages of mammalian P1 as proposed by Balhorn (1). The two intramolecular disulfide linkages which are between cysteine 6, 14 and 39, 47 are responsible for the curving of the molecule. The three intermolecular disulfide linkages help in the formation of nucleoprotamine and interprotamine interactions.

The three intermolecular disulfide linkages crosslink neighboring protamine molecules around the DNA helix. Thus, out of the seven cysteines that are present in bull protamine P1, four participate in intramolecular disulfide bonds and three participate in intermolecular disulfide bonds.

The primary amino acid sequence of P2 has been reported for only three species which are shown in Figure 3 (1). The primary amino acid sequence of P2 from syrian hamster is incomplete. Unlike P1, P2 molecules are of variable length in various species and the sequence is not as conserved. P2 molecules are usually longer than P1. The arginines are more evenly distributed throughout the length of the molecule. They contain a high content of histidine while P1 molecules rarely contain histidines.

Gatewood et al.(4) studied the secondary structure transitions in human protamine P2 induced by zinc. They used circular dichroism (CD) to study the secondary structure of P2. Zinc is associated with human sperm physiology. Epididymal sperm contains less zinc, but the levels of zinc increase after exposure to prostatic secretions. The exact role of zinc is not clear. Removal of zinc by EDTA from sperm extract lead to the solubilization of sperm in SDS solutions without adding reducing agents. So the role of zinc was proposed to involve the blocking of free thiols thus reducing the disulfide cross-links formed. Later it was revealed that the sperm depleted of zinc upon storage became progressively more resistant to SDS solubilization.

RTHGQSHYRRRHCSRRRLHRHRRGHRSCRRRLRRSCRHRRRHRRGRTALRTCRR
H

Human protamine P2

RGQHHHRRRCSRRKLYRIHRRRRSCRRRRHSCRHRRRHRRGCCRS??RR?C

Hamster protamine P2

RGHHHHRHRRCSRKRLHRIHKRRRSCRRRRRHSCRHRRRHRRGCRRSRRRRRCR
CRKCRRHHH

Mouse protamine P2

Figure 3: The primary amino acid sequence of protamine P2 from human, hamster and mouse (1). They have more than 50 amino acids and are variable in length compared to each other. The arginine residues are evenly distributed throughout the length of the molecule. There are more than seven histidine residues present in each of them.

When zinc was added to P2 in solution, there was a change in CD spectra at 197 nm. This was not an ionic effect since magnesium or calcium did not induce a similar change. Upon addition of 1 nM zinc, the magnitude of the minima at 197 nm decreased by 44%. They used the CD analysis method developed by Hennessey and Johnson, and proposed a model for zinc - protamine complex as shown in Figure 4. They concluded that human P2 in Zn / NaCl has 70% turns, 11% anti-parallel β-sheet and 21% other protein structures. In the model, two zinc ions chelate protamine forming a zinc finger-like structure. This structure has positively charged loops that facilitate interaction with DNA and the hydrophobic pockets that are formed by the residues surrounding the zinc ion. But, this type of structure is possible only with those protamines that contain histidines and cysteines. Although mammalian protamines contain histidine and cysteine, other vertebrate protamines, like salmon for example, do not contain these two amino acids. So, the structure of protamines and nucleoprotamines might be different in mammals and fish. Other structures also might be formed by the protamine - zinc complex. Zinc may also serve to crosslink the repeating units of nucleoprotamine into higher order structures. There are 4 cysteine and 1 histidine residues in human protamine P2, which are free to interact with the adjacent protamine molecule via disulfide bond or zinc bridges. There are a total of nine histidines in human P2, eight of which are involved in intramolecular zinc chelation as shown in Figure 4.

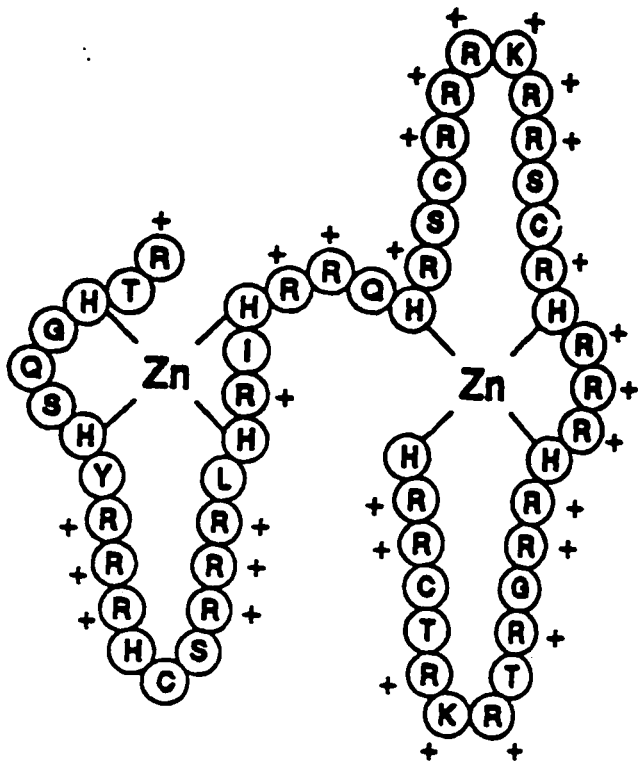

Figure 4: Proposed structure for human protamine P2-zinc complex. Gatewood et al. (4) proposed the above structure for the P2-zinc complex based on the data obtained from circular dichroism studies and structure predictions. The complex involves the chelation of two Zn+2 ions by P2, consisting of loops of highly charged arginine residues looping away from the hydrophobic zinc coordination.

Formation of nucleoprotamine

In somatic cells, histones cause the condensation of the DNA, forming nucleosomes. During the late stages of spermiogenesis, histones are replaced by protamines forming a nucleoprotamine complex. The formation of nucleoprotamine depends on the types of protamine involved in the process and is species specific. Electron microscopy studies showed three structural states of chromatin during the spermatid maturation (2) in many species. The spermatids in the early stages of development are round and are organized by nucleosomes. In the later stages, the spermatids are elongated, consisting of non-nucleosomal chromatin with thin, smooth filaments of nucleoprotamines. There is a transition state consisting of both nucleosomal and smooth fibers in the early stages of elongate spermatids.

Marushige and Marushige (5) studied the formation of disulfide bonds in protamines (historically called sperm histones) and the maturation of spermatids in rat. The number of cysteine residues involved in disulfide linkages in protamine were determined for various dissected regions in the reproductive tract such as testis chromatin, caput, cauda epididymal spermatozoa, and mature rat spermatozoa (Figure 5). Their studies showed that all the cysteine residues of protamine in testis chromatin are present as free sulfhydryl groups. All the cysteines of protamine in cauda epididymal spermatozoa and mature spermatozoa are involved in disulfide linkages. Approximately half the cysteine residues of protamine in caput epididymal spermatozoa are involved in disulfide linkages.

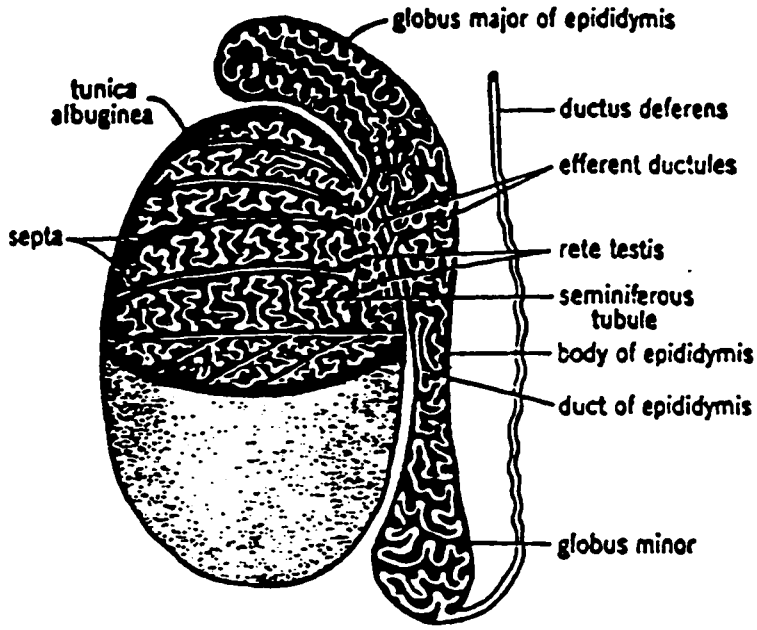

Figure 5: Diagram of the testis with epididymis of the male rat (6).The spermatids that arise in testis go through physiological and morphological changes into mature sperm as they move from testis through different parts of epididymis. In the diagram, the caput epididymis is represented as the globus major and cauda epididymis as the globus minor of the epididymis. The corpus epididymis is the body of the epididymus.

These results suggest that the formation and stabilization of nucleoprotamines takes place by crosslinking of protamines through the formation of disulfide bonds during the passage of the spermatozoa through the epididymis.

Phosphorylation and dephosphorylation of histones and protamines also play an important role in the formation of nucleoprotamines. Louie and Dixon (7) studied the synthesis and extent of phosphorylation of histones and protamines in various stages of spermiogenesis in trout testis using [^{3}H]arginine or lysine, inorganic phosphate and sedimentation techniques. Their studies showed that the protamines are synthesized during the middle spermatid stage in trout. The newly synthesized protamines are extensively phosphorylated and replace the histones. The protamines bind to the chromatin causing the initial condensation in the middle spermatid stage. Later the histones are released, probably by acetylation, in the late spermatid stage (8). Further condensation of the chromatin by protamines into nucleoprotamine is facilitated by controlled dephosphorylation. Thus phosphorylation may be important for the initial binding of protamine to the DNA and dephosphorylation is connected with the final condensation of the DNA. Thus the phosphorylation and dephosphorylation processes are important for the proper binding of the protamine with the chromatin and then cause the condensation.

The formation of nucleoprotamine takes place in different ways in clupeine (herring protamine), eutherian mammal and human sperm. Bode et al. (9) studied the release of histones by addition of clupeine using native and conventional chromatin

preparations and a fluorescamine assay. Their studies showed that protamines exhibit a stronger electrostatic interaction with DNA compared to histones. Thus when nucleoprotamines are formed, histones cannot replace protamines unless histones are present in large excess. They proposed that protamines compact DNA by crosslinking the histone-depleted regions, initiated by protamine phosphates that form salt bridges with arginines to give a loose and large network. They suggested that acetylation of histones (9) and dephosphorylation of protamines play an important role in the formation of nucleoprotamine complexes.

In eutherian mammals, like mice and rats, histones are present till the late spermatid stages (2). In late spermatid stages, the histones are replaced by low molecular weight transitional proteins. Protamines finally replace the transitional proteins, and cause the compaction of DNA by phosphorylation and dephosphorylation of the protamine. The nucleoprotamines are stabilized by the formation of disulfide crosslinks between the protamine molecules. The sperm of many mammals appear to lose all the histones during the formation of nucleoprotamine. But mature human sperm retain about 15% of the histones (2).

In human and mouse sperm, protamine P2 is synthesized as a longer precursor and incorporated into the spermatid. The P2 precursor is deposited on the DNA, and later undergoes several proteolytic cleavages to yield the final form of P2. Radiolabeling studies showed that the proteolytic cleavage of P2 precursor occurs in an ordered fashion and

each intermediate persists for several hours. Both the precursor and the final form of P2 are phosphorylated (1).

Structural aspects of nucleoprotamine

Atomic force and electron microscopy results (10) suggested that the bulk of the DNA is arranged as a close packed arrangement of protamine-DNA toroids. Each toroid has approximately 60 kbp of DNA, ~900 A^0 outside diameter, 200 A^0 thick, and has a 150 A^0 diameter hole. Considering the calculated content of DNA in a toroid and the size of mammalian haploid genome, it was estimated that each sperm nucleus contains about 50,000 closely packed toriods with uncoiled regions of DNA acting as links between neighboring toroids.

Many studies were conducted to study the structure of the nucleoprotamine complexes. X-ray diffraction studies by Subrina and Suan (11) suggested that the protamine was located in the minor groove of the DNA. Subrina and Suan studied the complexes formed by DNA and different types of protamine by X-ray diffraction. They used protamines from different species with various amino acid compositions. Differences in size or amino acid composition of protamines did not have an influence on the diffraction patterns obtained for nucleoprotamine complexes. At 76% humidity, the DNA in the nucleoprotamine was in B form. At lower humidity, the DNA was slightly distorted but did not show transition to any other form. From the X-ray diffraction patterns, they concluded that the location of protamine is in the minor groove of B form DNA.

Mirzabekov et al.(12) concluded that the protamine is associated with the major groove of DNA after testing the chemical reactivity of nucleoprotamine. Raman spectra studies by Mansy et al. (13) suggest that the arginine residues of protamine interact with guanine in the major groove of DNA. Fita et al. (14) conducted the studies using X-ray diffraction and concluded that the arginines are located on the major groove of DNA. They also found that the DNA was in a stable B conformation with ten base pairs per helical turn in all the complexes with different polyarginine proteins and under all humidity conditions. The guanidinium moiety of arginine can form hydrogen bonds with two consecutive phosphates. This feature stabilizes the B-conformation of DNA even in the absence of water.

Warrant and Kim (15) conducted single crystal X-ray diffraction of tRNA and circular dichroism studies of free protamine, and concluded that the conformation of protamine changes from a random coil to α-helical structures upon binding tRNA. They also concluded that the α-helical segment seemed to bind to the minor groove of the tRNA. But in their computer model for nucleoprotamine, the α-helical segments bind in the major groove of DNA.

Balhorn (16) proposed a model for the structure of nucleoprotamine based on the results from X-ray diffraction studies. In the model, the protamine binds in the minor groove of DNA. He suggested that the protamines either in α-helical or extended conformation can easily bind to both phosphate chains of DNA, if they lie in the minor groove. He proposed that the conformation of protamine in nucleoprotamine is not α-

helical as proposed by Warrant and Kim since calculations show the charged region of protamine (central polyarginine region) could span only half the length of DNA that is actually covered by protamine. If the entire protamine adopts an extended conformation, the length of protamine would be 2 to 3 times more than the length of the minor groove. So, he suggested that the central polyarginine segment is extended and binds within the minor groove, while the C-terminal and N-terminal residues are available for intra- and interprotamine interactions through hydrogen bonds or disufide linkages. One protamine molecule fills one turn of DNA and adjacent molecules are placed around the DNA by disulfide linkages.

Hud et al. (17) studied the DNA-protamine complex in the solid state using Raman spectroscopy at 98% relative humidity. Their data indicated the presence of a modified B-form DNA with some degree of base unstacking. They used salmon protamine (salmine) and polyarginine. Both showed similar results. The Raman spectra also presented a dominant amide I band for DNA-salmine complex. This band is not consistent with an α-helix or β-sheet conformation of salmine, but suggests the presence of a novel secondary structure. The results also indicated that both salmine and polyarginine underwent conformational changes upon binding to DNA. Based on these results, Hud and coworkers proposed a new model of the protamine-DNA complex. In this model, protamine is bound within the major groove of the DNA and not in the minor groove as proposed earlier. The backbone conformation of the protamine facilitates intramolecular hydrogen bonding between neighboring arginines in each cluster.

Bianchi et al. (18) studied the interaction of DNA fragments of 802, 448, 226, 102 and 48 base pair in length with human protamines P1 and P2 using a gel mobility shift assay. They observed a complete shift in mobility due to precipitation for all the lengths of DNA used, at arginine to phosphate ratio of 0.1 with both with P1 and P2. At an arginine to phosphate ratio of 0.5, partial precipitation of the DNA-protamine complexes occurred whereas, at 1.2 ratio, total precipitation occurred. Both P1 and P2 behaved similarly in the gel mobility shift assay. Table 1 shows the results from the gel mobility shift assay. They also conducted the same experiment with and without $ZnCl_2$ to study the effect of zinc on the binding of DNA to protamines. The results showed that with or without Zn^{2+}, there was a complete shift at an arginine to phosphate ratio of 0.1. They also studied the effect of NaCl concentration on DNA - protamine complexes. As the concentration of NaCl was increased from 0.2M to 0.7M, the amount of DNA complexed by protamine molecules decreased, which indicates that electrostatic interactions are predominant. Additionally, they used the dye Hoecht 33258 with DNA and fluorescence spectroscopy to determine the location of binding of protamine to DNA. The dye binds in the minor groove of DNA and becomes brightly fluorescent upon binding. When protamines were added to DNA, the fluorescence intensity increased and reached a plateau at arginine to phosphate ratio of 1.2. This suggests that protamines do not displace the dye from the minor groove of DNA since they do not bind within the minor groove of DNA. From these experiments they concluded that human protamines form a complex at low arginine

		Double stranded DNA					
Protamine	**Zn**	**48**	**102**	**222**	**266**	**448**	**802**
HP1	+	0.1 ± 0.02	0.1 ± 0.02	0.08 ± 0.02	0.09 ± 0.02	0.1 ± 0.02	0.11 ± 0.02
HP1	–	0.09 ± 0.02	0.1± 0.02	0.1± 0.02	0.08 ± 0.02	0.1± 0.02	0.11 ± 0.02
HP2	+	0.09 ± 0.02	0.12 ± 0.03	0.1± 0.02	0.1± 0.02	0.1± 0.02	0.1± 0.02
HP2	–	0.09 ± 0.03	0.12 ± 0.03	0.1± 0.02	0.1± 0.02	0.11 ± 0.02	0.1± 0.02

Table 1: Electrophoretic mobility of human protamines P1 and P2 complexed with different DNA fragments, in the presence and absence of Zn in a mobility shift assay. The fractions given in the table represent arginine to phosphate ratio at which a complete shift in the mobility was observed. Mean ± standard deviation of 3 experiments was given (18).

to phosphate ratios. Protamines have the capacity to bridge several DNA fragments. They concluded that protamines do not bind within the minor groove of DNA. Instead, they suggested that DNA either folds around protamine or a parallel arrangement of DNA and protamine molecules occur. P1 and P2, though structurally different, showed functional equivalence with regard to their DNA bonding properties. Zn^{2+} did not appear to play a role in DNA - protamine interactions, though Zn^{2+} is believed to stabilize P2 secondary structure via formation of a Zn - finger structure (4).

Thus, a significant number of experiments were conducted using different techniques, by different groups, to study whether protamines bind in the major or minor groove of DNA. The majority of the studies conducted support that protamines bind in the major groove of the DNA. Most of the studies used P1 in their experiments. Bianchi et al. (18) used both human P1 and P2, and concluded that P1 and P2 show similar binding characteristics with DNA, though they are structurally different.

Models for the cooperative binding of Protamines to DNA

McGhee and von Hippel (19) presented a mathematical approach to the interaction of protamines binding non-specifically to DNA. They considered DNA as a homogeneous lattice which was taken as a linear array of identical repeating units. The repeating units correspond to the base-pair or phosphate backbone of DNA. The ligand molecule, which is the protamine, was assumed to bind to DNA and cover "n" consecutive lattice residues.

They considered that the lattice is oriented in one particular direction and that the ligand binds in a fixed orientation with respect to the lattice. Ligand - ligand interactions are allowed between nearest neighbors which give rise to three types of ligand - ligand sites. They are, "isolated" sites, "singly contiguous" sites and "doubly contiguous" sites. The co-operativity parameter is defined as ω. If ω is greater than 1, the ligands attract each other. If ω is less than 1, it is called negative co-operativity, where the ligands repel each other. If ω is equal to 1, it is non-cooperative binding. For an isolated site, the association constant is $K(M^{-1})$. For a single contiguous site, the association constant is $K\omega(M^{-1})$, and for double contiguous site, the association constant is $K\omega^2(M^{-1})$. They have derived equations to describe both co-operative and non-cooperative binding of any size ligand to a homogeneous or heterogeneous lattice. From their equations, they suggested that the lattice resists being saturated entropically. Full saturation of the lattice can only be achieved by increasing the concentration of free ligand or by increasing the ligand-ligand affinity (increasing ω).

Watanabe and Schwarz (20) studied the thermodynamics and kinetics of cooperative protamine-nucleic acid binding. The protamine used was a fluorescein labeled clupeine Z (herring protamine). They used fluorescence titration methods and chemical relaxation techniques for the study. They proposed a model for co-operative binding which implicates two types of elementary binding steps. One is ligand binding to a site whose neighboring polymer subunits are empty and the binding constant is K. The second is the ligand binding to a site immediately adjacent to the occupied site and the binding

constant for this is K'. The parameter q =K/K', gives the co-operativity between adjacent bound ligands.

Using a kinetic approach, Watanabe and Schwarz determined the rate constant for the dissociation of the DNA-protamine complex. They tested the effect of different concentrations of NaCl by suddenly mixing the DNA-protamine solution in different NaCl concentrations. Upon decreasing [NaCl], they observed a decrease in K_D which may be due to an increase in electrostatic activation energy. They have observed an increase in the cooperativity parameter upon an increase in [NaCl]. Based on their results, they proposed a hypothesis for the cause of cooperativity. They proposed that the negative charges of DNA are neutralized by protamine molecules. So at protamine binding sites, there is no ionic cloud of negative charge. There is a dispersal of negative cloud on the unoccupied binding site adjacent to the protamine bound sites which, as a result will be screened to a lesser extent electrostatically by the approaching protamines than those far away. So, this enhances the binding and increases the binding constant in the neighborhood of protamine bound sites.

Willintzer and Wagner (21) studied that effect of NaCl concentration on the binding of calf thymus DNA and culpeine Z. They suggested from their studies that the observed cooperativity is due to cross linking of protamines around DNA molecules. They concluded that electrostatic forces are involved in the binding of DNA with protamines. There is a competition between arginines of protamines and sodium cations for the negative charges on the phosphate backbone of DNA.

However, in the present study, a low protamine substitution on resin was used. It is unlikely any cooperativity between the protamine molecules will exist since the protamines will be far apart.

Significance of P2

The two types of protamines, P1 and P2, are present in different proportions in various species. For example mouse sperm has twice the amount of P2 as P1, whereas hamster sperm has twice the amount of P1 as P2. They perform similar functions, like the condensation of DNA in sperm cells in all the species inspite of the variation in the proportions of these two protamines. This suggests that the two protamines may be used interchangeably in sperm chromatin (1). But the structural features of these protamines are different, and they may interact differently with other proteins or ligands. For example, P2 has a high histidine content compared to P1. Histidines as well as cysteines coordinate with other proteins or metal ligands. Studies have shown that P2 plays an important role in sperm chromatin organization and fertility in humans (1). It was observed that the proportion of P2 was markedly reduced in sperm from infertile males and they have an elevated level of large sperm heads.

Yerba et al.(22) conducted an analysis of the nuclear proteins of 116 sperm samples from different infertile humans. They analyzed the ratio of different types of protamines in the sperm. They observed that 112 sperm samples out of 116 have a decrease in the level of P2, whereas four sperm samples showed complete selective

absence of P2. This complete absence of P2 could be directly or indirectly responsible for the male sterility. The complete absence of P2 could arise from a lack of expression of the P2 gene or due to irregularities in its processing, transfer into the nucleus, or binding of P2 precursor to the DNA. They sequenced the P2 genes to search for mutations. No mutations were found in the coding region or in the promoter up to 200 base pairs from the transcriptional start site. They suggested that some diseases like infections, immunological changes, and hormonal changes affect spermatogenesis which could lead, through an independent mechanism, to the alteration of the levels of P2 or complete selective absence of P2. Thus, selective absence of P2 should lead to a loss of biochemical, structural, and functional aspects provided by P2.

Studies have also shown that the presence of P2 alters the way the protamines interact with each other. For example, in species like hamster that contains both P1 and P2 molecules, P1-P2 molecules do not occur as dimers. P1 or P2 molecules cannot be extracted from a sperm unless the sperm is first reduced, which suggests that disulfide linkages play an important role in the interprotamine interactions between P1 and P2. On the other hand, the isolation of distinct P1 dimers from bull sperm which does not contain P2, suggests that the P1 molecules may be bound to DNA as a dimeric unit. The P1 molecules in the dimers cannot possibly be linked through disulfide linkages because the dimers are stable in boiling mercaptoethanol. The linkage between the two molecules is susceptible to HCl which suggests that the two molecules could be linked through an ester linkage.

Approaches to kinetic studies of protein-DNA interactions

In the present study, the dissociation rate constant, k_2, for the DNA-protamine P2 complex was determined. Determination of the k_2 of complex dissociation requires the separation of free and bound components. Usually, one of the following three methods have been used to determine the ratio of bound to free ligand: equilibrium dialysis, centrifugation, and vaccum filtration. Equilibrium dialysis is used in the case of low affinity complexes with a dissociation constant, K_D of 10^{-3} M. Highly charged molecules like polynucleotides cannot be used because they may stick to surfaces and the determination of the ratio of bound to free ligand becomes difficult. For moderate affinity complexes (K_D 10^{-5} M), centrifugation can be used to separate the free and bound ligands. The bound ligand is usually pelleted and the free ligand is in the supernatant. This method is rapid in suitable conditions. Filtration techniques are used for high affinity complexes (K_D $<10^{-8}$ M). Dissociation of the DNA-protamine complexes require severe conditions. Gatewood et al. (23) isolated histones and protamines separately from human sperm. At 0.65M NaCl, the nucleohistone complexes decondensed, whereas the nucleoprotamine complexes decondensed at 0.95M NaCl.

A combination of centrifugation and filtration was used by Wren (24) to study the kinetic aspects of the interaction of DNA and bull protamine P1. She used thiol activated Sepharose resin as a solid substrate to immobilize the protamine. P1 was substituted on sepharose resin via a disulfide exchange reaction. Radiolabeled DNA was added to the

immobilized P1 to detect complex formation. After a 100-fold dilution of the complexes, centrifugation was used to determine the free [DNA] and filtration was used to determine the bound [DNA]. The resin with associated DNA-P1 complexes was retained by nitrocellulose filters. Liquid scintillation counting was used to quantitate the free and bound radiolabeled DNA. The DNA-P1 complex appears to be a high affinity complex. The dissociation rate constant determined for a 12 base pair DNA-P1 complex in 0.1 M NaCl, 50 mM HEPES pH 7.5 was $8.9 \pm 4.4 \times 10^{-5}\ s^{-1}$, which gives a half-life equivalent to 117 minutes. As the concentration of NaCl was increased, the dissociation rate constant also increased, suggesting that electrostatic forces are involved in the binding of DNA to P1. An increase in the dissociation using 10 base pairs of DNA as compared to 12 and 14 base pairs of DNA , suggests that the number of base pairs of DNA is an important factor in the affinity of the DNA-P1 complexes.

Another solid substrate which can be used to immobilize macromolecules are dynabeads™. Dynabeads™ (Dynal) are uniform, paramagnetic, polystyrene beads that are coated with a polyurethane layer (manufacturer). An even dispersion of Fe_2O_3 is coated with a thin polystyrene shell. The polystyrene shell provides a defined surface area for the adsorption and coupling of various molecules, and protects the target from toxic exposure to iron. Uniformity of the beads provide consistent chemical and physical properties, and also provides optimal reaction kinetics between the dynabeads and the target. The uniform spherical shape eliminates clumping and nonspecific binding.

Proteins may be attached to tosylactivated dynabeads. The amino group of the N-terminal amino acid of the protamines or the sulfhydryl group of cysteine displaces the tosyl group on the beads and covalently binds to the beads. There was no information found in literature on the use of the M-280 tosylactivated dynabeads to study the kinetics of DNA-protein interactions. However, information was found in the literature on the use of M-280 tosylactivated dynabeads in the separation of specific cell types (25, 26) and protein purification. Jackson et al. (25) used tosylactivated dynabeads for the isolation of human microvascular endothelium from rheumatoid arthritic and osteoarthritic synovial tissues. Previous purification techniques used were weeding and sorting by flow cytometry, which required a large number of endothelial cells. Microvascular endothelium cells have limited replication capacity and contaminating cells such as fibroblasts grow rapidly and overgrow endothelial cells. Jackson and coworkers devised a method for the purification of endothelial cells in which lectin Ulex europeaus I (UEA I) was covalently bound to the tosylactivated dynabeads. UEA I binds selectively to endothelial cell surface via fucose residues. The attachment of UEA I particles to the cell surface membrane of endothelial cells can be visualized using scanning electron microscopy. The endothelial cells immobilized on the dynabeads can be plated on gelatin coated dishes and the dynabeads did not interfere with the physical behavior of normal replication of the endothelial cells. The endothelial cells can be separated from the dynabeads without effecting their cellular behavior, by competitive binding with fucose.

Dynabeads can also be used for immunoseparation assays. Gladwin et al. (26) developed a simple method to separate intact megakaryocytes from whole bone marrow using goat-anti-mouse IgG coated dynabeads. Using the immunomagnetic separation method, the purity of the megakaryocytes obtained was > 98%. Electron microscope examination of the purified megakaryocytes showed that their ultra structure was well preserved. Megakaryocytes immobilized on the dynabeads were further used to isolate platelet-derived-growth-factor (PDGF) mRNA. They performed the hybridization of PDGF mRNA with radiolabeled riboprobe obtained from B-chain of human megakaryocytes. The riboprobe was obtained by the transcription of human DNA sequence containing sis sequence from the SP6 promoter by using [^{32}P] UTP and SP6 RNA polymerase. The results suggest that the B chain of PDGF may be synthesized in human megakaryocytes and it is one source of PDGF found in platelets. Thus, in the above two applications dynabeads not only enabled a simple and efficient purification of the required cells, but also did not interfere in the later procedures during the utilization of the immobilized cells.

Dynabeads can also be used for protein purification. For protein purification, dynabeads are coated with a primary antibody against the protein to be purified from a heterogenous protein mixture. In these assays, dynabeads are coated with an antigen and are used to isolate specific antibodies of those antigens. In some cases they are coated with antibody and are allowed to react with the antigen. The antibody-antigen complexes

can be detected by radioactive labeling, fluorescent substances, enzymes, or chemiluminescence.

Dynabeads coated with streptavidin are available to which biotin-labeled DNA oligomers can be attached. Those transcription factors which bind more strongly to a specific DNA sequence than to other DNA sequences can be isolated and purified by using the specific DNA sequences immobilized on dynabead streptavidin. This approach to the purification of transcription factors is more rapid than DNA affinity chromatography. Gabrielsen et al. (27) used streptavidin dynabeads to purify yeast transcription factor within 30 minutes. Double stranded plasmid DNA can also be immobilized on streptavidin dynabeads and used for sequencing reactions (28). Amplified plasmid DNA or chromosomal DNA from the PCR reaction can be immobilized on the streptavidin dynabeads by using one biotinylated primer in PCR reaction, out of the two primers being used. The immobilized single strand template for the sequencing reaction can be obtained by strand-specific elution. Streptavidin dynabeads can be used both with fluorescent and radiolabeled primers.

In the present case, DNA was not immobilized on the dynabeads in order to avoid the use of streptavidin which may affect protamine binding. So, M280-dynabeads tosylactivated reacted with protamines P1 or P2 were used to test the suitability of the system to study DNA-protamine interactions.

Objectives of the project

There are three objectives to the project. The first objective is to establish the tosylactivated dynabeads™ as a solid substrate method to examine DNA-Protamine interactions. The second objective is to determine the dissociation rate constant and the half-life of the DNA-protamine P2 complex under specified conditions using tosylactivated dynabeads. The third objective is to determine the effect of different concentrations of NaCl on the dissociation of DNA-P2 complexes.

In the experiments performed to fulfill these objectives, bull protamine P1, hamster protamine P2, and 12 base pair DNA oligomers were used. The protamines were substituted on the dynabeads by the replacement of tosyl groups of the dynabeads by the N-terminal amino group of the protamine or the sulfhydryl of cysteine present in protamine. Radiolabeled DNA was then added to the protamines to form DNA-protamine complexes. The free DNA and the DNA bound to protamine were separated with the help of a Magnetic Particle Concentrator (MPC). Paramagnetic dynabeads will stick to the wall of an eppendorf tube in a MPC, and the supernatant containing free DNA can be easily removed. The free and bound radiolabeled DNA were quantitated using the liquid scintillation counter.

In this project, a procedure for immobilization of protamines on dynabeads was established. The dissociation rate constant and half-life of DNA-P2 complexes were

determined using the dynabead system. The effect of the concentration of NaCl on the DNA-P2 complexes was determined.

MATERIALS AND METHODS

Buffers

The buffers used for the preparation of solutions in the experiments were HEPES and TAPS buffers. The HEPES buffer was prepared by mixing HEPES-acid, and its sodium salt. Fifty mM HEPES-acid and HEPES-Na salt were prepared and mixed to yield pH 7.4. The TAPS buffer was comprised of TAPS-acid, and its sodium salt. Fifty mM TAPS-acid and TAPS-Na salt were prepared and mixed to obtain pH 9.5. All buffers were purchased from Sigma and Aldrich. The 10 mM HCl was prepared volumetrically in water. The NaCl solutions, 0.1, 0.2, 0.25, 0.3, 0.5 and 1 M were prepared in 50 mM HEPES volumetrically.

DNA Labeling

Twelve base pair DNA oligomers were synthesized chemically by Clonetech. Complementary single strands were prepared, purified by reversed phase high performance liquid chromatography (HPLC), annealed to yield double stranded DNA oligomers, and purified by reversed phase HPLC by Mr. Joe Mazrimas (Lawrence Livermore National Laboratory). The double stranded oligomers were deblocked to leave 5'-OH groups.

The concentration of the DNA oligomers was determined by UV absorbance at 260 nm. The extinction coefficient used was 20 cm^2/mg. A Hewlett Packard Diode Array

Spectrophotometer, model 8452A, was used. The spectral bandwidth for the instrument is 2 nm.

The sequence of the 12 base pair DNA oligomer was:

5'-OH-TC-GAA-TGT-ACA-A-3'
3'-AG-CTT-ACA-TGT-T-OH-5'

T4 polynucleotide kinase (Kodak International Biotechnologies or Stratagene), was provided in 1 mM dithiothreitol, 0.1 mM EDTA, 100 mM NaCl, 50 mM Tris HCl (pH 7.5), 0.1% Triton X 100, and 50% glycerol. (One unit of activity is the amount of the enzyme required to catalyze the incorporation of 1 nmole of phosphate from [^{33}P-γ]ATP onto the 5'end of the DNA oligomer at 37 ^{0}C in 30 minutes). The tenfold stock concentration of the reaction buffer C contained 500 mM Tris HCl, 10 mM EDTA, 1 mM spermidine, 50 mM dithiothreitol and 100 mM $MgCl_2$.

An aqueous solution of [^{33}P-γ]ATP was obtained from NEN Research Products, Dupont. It contained 4500 Ci/mmol, 0.25 mCi/0.025 mL in 10 mM tricine at a specified date by the manufacturer.

The 12 base pair double stranded DNA oligomers were labeled with [^{33}P-γ]ATP according to the protocol of Lillehaug et al. (29) using the enzyme T4 polynucleotide kinase. A 20 μL solution containing 100 pmol of DNA ends in 1 μL of 50 mM HEPES,

20 μCi (2 μL) [^{33}P-γ]ATP and approximately 10 units of T4 kinase was prepared. Addition of T4 kinase initiates the reaction. The mixture was incubated at 37 ^{0}C for 45 minutes in a water bath. After 30 minutes on ice, 30 μL of 50 mM HEPES was added.

Quickspin™ gel permeation columns were used to separate the labeled and unlabeled DNA from unreacted [^{33}P-γ]ATP in the mixture. The Quickspin™ gel permeation columns containing fine Sephadex G-25 in 0.1 M NaCl, 10 mM Tris HCl and 1 mM EDTA were obtained from Boehringer Manheim. According to the manufacturer, the exclusion limit of the columns is 10 base pairs of DNA, recovery of DNA bigger than 10 base pairs is 80%, and the retention of molecules smaller than 10 base pair DNA is 95%. Prior to use, the Quickspin™ columns were buffer exchanged with 50 mM HEPES by washing the columns with 500 μL 50 mM HEPES and centrifuging. This was performed four times at 800g for 2 minutes and the final time at 400g for 2 minutes. The separation of unreacted label occurred by addition of the reaction mixture to the buffer equilibrated Quickspin columns and centrifugation at 400 g for 2 minutes.

The radioactivity of the samples before and after separation by the Quickspin column was quantitated by liquid scintillation counting in Cytoscint (ICN). A Packard Tri-Carb Liquid Scintillation Analyzer, model # 1900CA was used to detect the radioactivity. Three regions A, B, and C were set over the stored spectrum to form regions of analysis in the Liquid Scintillation Analyser. These regions were automatically defined of ^{3}H, ^{14}C, ^{32}P, and ^{125}I in single label measurement. The windows were set at 5.0-1700 for Region A, 50.0-1700 for Region B and 0-0 for Region C and 2σ% for all the regions was at zero.

The percentage of recovery of radioactivity into labeled DNA and the specific activity of the labeled DNA were calculated. The total label in the effluent recovered varied anywhere from 25 to 40%.

Protamine substitution on dynabeads

Both bull protamine 1 (P1) and hamster protamine 2 (P2) were isolated, purified and supplied to us by Dr.Balhorn (Lawrence Livermore National Laboratory). P1 was isolated from bull semen whereas P2 was isolated from hamster semen by Mr. Joe Mazrimas using a nickel column (personal communication). They were purified by reversed phase HPLC. P1 was stored in lyophilized form, whereas P2 was stored in 10 mM HCl at -20 ^{0}C.

The molecular weight of bull P1 is 6640 Da (23). The concentration of the P1 solution in 10 mM HCl was determined by UV absorbance at 230 nm using the molar extinction coefficient of 38,500 M^{-1} cm^{-1}(Dr. Balhorn, personal communication). The molecular weight of hamster P2 used was 7622 Da .(The molecular weight of the three unknown amino acids was taken as 110, which is the average molecular weight of the amino acids.) The concentration of P2 solution in 10 mM HCl can also be determined by UV absorbance at 230 nm wavelength. The extinction coefficient is 4.8 cm^2/mg (Dr. Rod Balhorn, personal communication). The molar extinction coefficient of the P2 solution was calculated to be 36,600 $M^{-1}cm^{-1}$.

Dynabeads M-280 (Dynal) are uniform, paramagnetic, polystyrene beads which are coated with a polyurethane layer (manufacturer). They consist of an even dispersion of Fe_2O_3, coated with a thin polystyrene shell. These beads are activated by p-toluenesulphonyl chloride which facilitates the covalent binding of proteins. The amino group of the N-terminal amino acid of the protamines and the sulfhydral group of cysteine residues displaces the tosyl group on the beads and covalently binds with the beads at alkaline pH. The schematic diagram of the attachment of the primary amino group to the dynabeads is shown in Figure 6.

According to the manufacturer, the diameter of dynabeads M-280 is 2.8 μm ± 0.2 μm, the surface area is 4-8 m^2/g and the density is 1.3 g/cm^3. They are supplied as ethanol washed beads in aqueous suspension. Dynabeads can be separated from the solution by using the Magnetic Particle Concentrator (MPC). When an eppendorf tube with the bead solution is placed in a MPC, the beads will stick to the walls of the tube which is adjacent to the magnet. The supernatant can be easily removed without losing the beads. Then the tube is taken out of the MPC, the required solution is added, and the beads will resuspend.

The procedure followed was recommended by the manufacturer. The concentration of the dynabeads solution was approximately 10 mg/mL. Two hundred microliters of the solutions was taken (2 mg beads) and the beads were washed twice with 50 mM TAPS buffer (9.5 pH). TAPS buffer was used in the procedure for the solubility of protamine though it was not recommended by the manufacturer. After the second wash,

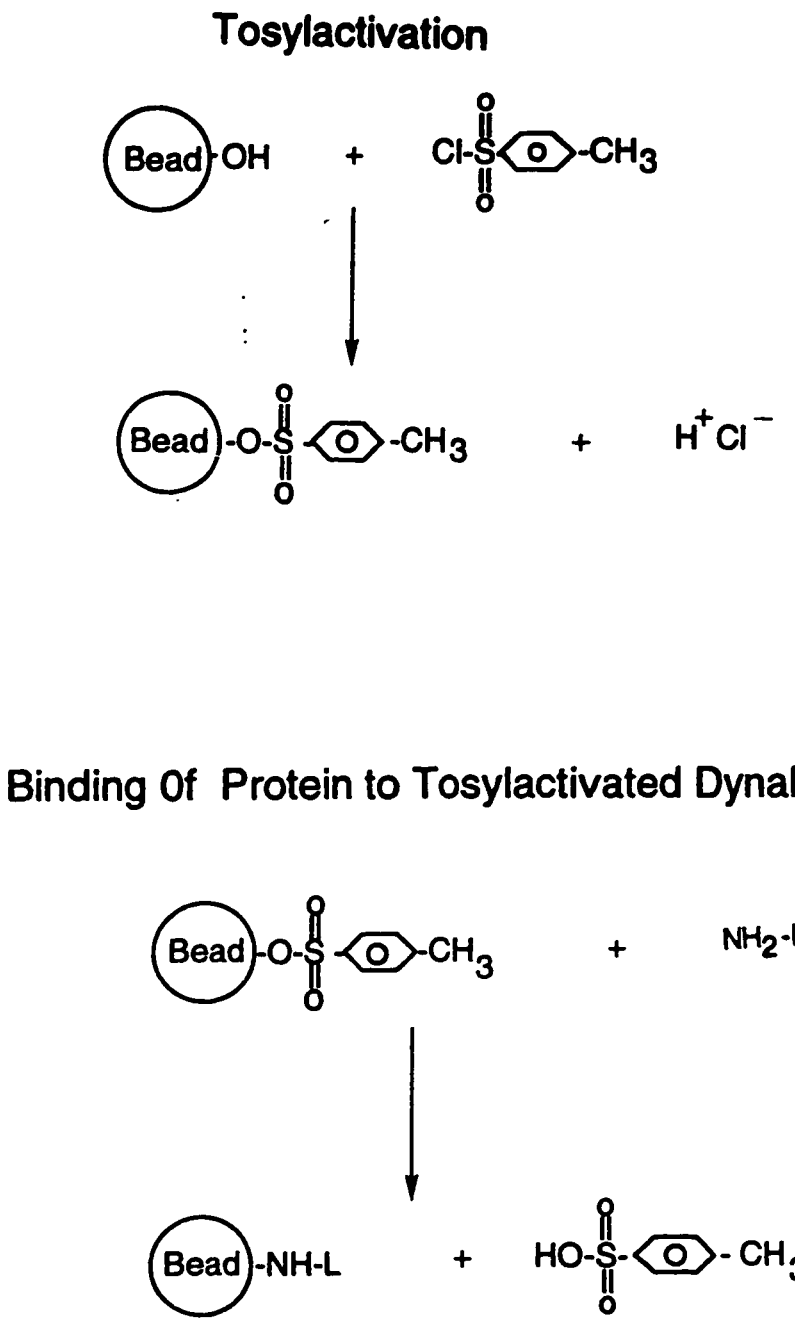

Figure 6: Tosylactivation and binding of proteins to tosylactivated dynabeads. In tosylactivation, the primary -OH groups on the bead surface react with tosylchloride forming a super-reactive tosyl group. These super-reactive tosyl groups react with the primary amino groups on the proteins. The tosyl groups are washed away after the binding of proteins to the bead surface.

the supernatant was removed, and 2 mg beads were incubated with 63 nM protamine in 50 mM TAPS at pH 9.5. This solution was incubated at 37 ^{0}C in a shaker at 160 rpm for 24 hours. At this temperature and pH (9.5), the beads will covalently bind the protamines. After the 24 h incubation, the beads were washed thrice for 10 minutes at each washing, and once for 30 minutes with 50 mM TAPS buffer. After the last wash, the supernatant was removed and 500 μL of the 50 mM TAPS was added. This solution was kept in the refrigerator at 4 ^{0}C overnight. After the overnight incubation, the beads were washed thrice for 10 minutes at each washing with 50 mM TAPS buffer. After the last wash, the supernatant was removed and 500 μL of 0.1 M NaCl, 50 mM HEPES solution (pH 7.4) was added. The same procedure was followed for preparing the control dynabeads except that no protamine was added. The same protocol was followed for substituting P2 onto the dynabeads, except different concentrations of P2 ranging from 63 nM to 630 nM were used.

Dissociation protocol

Complex formation of P1-DNA complexes takes place by mixing 500 μL of the prepared dynabead solution (control or P1-substituted beads), with 2 μM to 8 μM of ^{33}P-labeled DNA and incubated for 1 hour at room temperature with occasional shaking. The amount of DNA that would have 50,000 cpm was added for each 20 μL aliquot of the dynabead solution.

Dissociation of P1-DNA complexes was accomplished by a 50 fold dilution of the solution. After the one hour incubation, the DNA-protamine solution was mixed gently to obtain an uniform solution. This solution was then diluted 50 fold by taking 20 μL aliquots in eppendorf tubes and adding 980 μL dissociation buffer (50 mM HEPES, 0.1 M NaCl). The dissociation tubes were incubated for 0, 15, 30, 45 minutes, and 1, 2 , 3, 4 and 24 hours.

After the incubation for the required time, each tube was placed in the magnetic particle concentrator and allowed to stand for 1 min. Then 100 μL of the supernatant was removed into a scintillation vial containing 5 mL cytoscint fluid to determine counts per minutes (cpm) of unbound or free DNA. The rest of the supernatant was discarded, leaving the beads in the tube. The tube was then taken out from the MPC and 100 μL of 50 mM HEPES buffer was added to the tube. It was shaken to resuspend the beads. This solution with resuspended beads was removed into a scintillation vial to determine cpm of bound DNA.

The above dissociation protocol was also performed with the control dynabeads to yield the amount of non-specific binding (DNA binding directly to the unsubstituted beads). Duplicate samples were taken at each dissociation time period and the average cpm of the two samples was used to determine the dissociation rate constants.

Protamine substitution on thiol activated sepharose resin

Thiol activated sepharose resin was obtained from Sigma. The resin has a glutathione 2-pyridyl disulfide substituted on the cyanogen bromide activated Sepharose 4B resin. The linkage of protamine to the resin takes place through the formation of disulfide bonds involving the sulfhydral groups of cysteine residues present in the protamine molecule. The resin releases 2-thiopyridine upon the formation of the disulfide linkage with the protamine (24).

About 50 mg of thiol activated sepharose resin was swelled at room temperature for one hour in 16 mL of 50 mM HEPES buffer. After one hour, the solution was centrifuged for 2 minutes at 400 g in order to separate the resin for the buffer. The supernatant was discarded and the resin pellet was transferred in to a eppendorf tube. To the pellet, 800 μL of 50 mM HEPES was added.

To the resin solution, 200 μL of protamine P2 solution was added resulting in an 63 nM P2 solution and incubated for one hour at ambient temperature. The solution was centrifuged for 15 seconds at 17000 g and the supernatant was discarded. A 0.5 mL solution of 5 M guanidinium hydrochloride in 50 mM HEPES was added to the resin and incubated for 5 minutes to remove any non-covalently bound P2. It was then centrifuged and the supernatant was discarded. The resin was washed twice with 50 mM HEPES, 0.1 M NaCl and made up to 1 mL using the same buffer. The same procedure was followed for preparing the control resin except that no protamine was added.

Complexes were formed by mixing 400 μL of the prepared resin solution

(control or P2-substituted resin), with 4 to 8 μM ^{33}P- labeled DNA and incubating for 1 hour at room temperature with shaking.

After the one hour incubation, the solution was mixed gently to obtain an uniform solution. This solution was then diluted 50 fold by taking 20 μL aliquots in eppendorf tubes and adding 980 μL dissociation buffer (50 mM HEPES, 0.1 M NaCl). The tubes were incubated for 0, 15, 30, 45 minutes, and 1, 2, 3, 4 and 24 hours.

After the incubation for the required time, each tube was centrifuged for 15 seconds at 17,000 x g. Then 100 μL of the supernatant was removed into a scintillation vial containing 5 mL cytoscint fluid to determine counts per minutes (cpm) of unbound or free DNA. The resin was resuspended in the solution using a 1000 μL pipette. The solution with the resuspended resin was removed with a 1000 μL pipette and filtered over a nitrocellulose filter pre-wetted with deionized water. The filters (type HAWP) have 0.45 μm pores, and were obtained from Millipore Corporation. The filter with the resin was removed into a scintillation vial containing 5 mL cytoscint to determine cpm of bound DNA.

The above dissociation protocol was also performed with the control resin at dissociation time periods 0 and 24 hours, which yielded the amount of labeled DNA binding non-specifically to the resin. Duplicate samples were taken at each dissociation time period and the average cpm of the two samples was used to determine the dissociation rate constants.

Effect of the concentration of NaCl on the dissociation of P2-DNA complexes

To determine the effect of the concentration of NaCl on the dissociation of P2-DNA complexes, the complexes were formed, diluted with 50 mM HEPES, 0.1 M NaCl and the extent of dissociation was measured by progressively increasing the concentration of NaCl. The concentrations of NaCl solutions used were 0.1, 0.2, 0.4, 0.6, 0.8 and 1 M. A 20 μL aliquot of the DNA-P2 (substituted on dynabeads) solution was taken in an eppendorf tube and diluted 50 fold by the addition of 0.1 M NaCl, 50 mM HEPES. The solution was shaken to obtain a uniform solution. The tube was then placed in MPC for one minute and 100 μL of the supernatant was removed into a scintillation vial (cpm of unbound DNA). The tube was then removed from the MPC and the beads were resuspended into the solution. To this solution 100 μL of 0.11 mmol NaCl solution was added and mixed gently resulting in a 0.2 M NaCl solution. The eppendorf tube was again placed in MPC and 100 μL of the supernatant was removed for radioactive determination (cpm of cumulative unbound DNA). The above process was repeated with the specified increasing concentrations of NaCl. Finally, when the concentration of NaCl in the solution was 1 M, 100 μL of the supernatant was removed for cpm of cumulative unbound DNA, the rest of the supernatant was discarded and the beads were resuspended and removed into a scintillation vial with 50 mM HEPES (cpm of bound DNA). The plot of the cpm of cumulative unbound DNA as a function of the concentration of NaCl showed the effect of different concentrations of NaCl on the dissociation of P2-DNA complexes.

Calculations and data analysis

The quantitation of the radioactivity associated with the free and bound DNA was performed by liquid scintillation counting. The percentage DNA bound can be calculated from the following equation:

$$\% \text{ DNA bound} = (C_b/(C_f+C_b))\text{x}100) \qquad \text{(equation 1)}$$

where C_b is the cpm for bound DNA (filter or MPC pellet) and C_f is the total cpm for free DNA (supernatant).

The cpm for various samples of the free and bound DNA were converted into the amount of total free or bound DNA, by using the specific activity of the labeled DNA.

$$\text{Specific activity} = \text{cpm of total labeled DNA} / 100 \text{ pmol DNA} \qquad \text{(equation 2)}$$

$$\text{pmol DNA recovered} = (C_f+C_b) / \text{specific activity} \qquad \text{(equation 3)}$$

$$\text{pmol DNA bound} = (\text{pmol DNA input}) (\%\text{DNA bound}/100) \qquad \text{(equation 4)}$$

In order to determine the concentration of the labeled DNA bound specifically to the protamine, the concentration of the DNA bound to the control, unsubstituted beads was subtracted from the total concentration of DNA bound to the protamine-substituted beads.

The model used to calculate the dissociation constant is as follows:

$$C_P + C_D \underset{k_2}{\overset{k_1}{\Longleftrightarrow}} C_{DP} \qquad \text{(equation 5)}$$

where C_P = concentration of unbound protamine

C_D = concentration of unbound DNA

C_{DP} = concentration of 1:1 complex of protamine and DNA

k_1= association rate constant

k_2= dissociation rate constant

The dissociation rate constant k_2 for the equation 5 can be determined from the following equation :

$$\frac{dC_{DP}}{dt} = - k_2 C_{DP} \qquad \text{(equation 6)}$$

Integration of equation 6 gives :

$$\ln \frac{C_{DPt}}{C_{DP0}} = - k_2 t = \frac{\ln B_t}{\ln B_0} \qquad \text{(equation 7)}$$

where C_{DPt} and B_t are the concentrations of bound DNA at any time t, and C_{DP0} and B_0 are the concentrations of bound DNA at 0 min.

The value for k_2 can be obtained from the slope of the plot of time versus $\ln B_t/B_0$

The slope was calculated by using a linear least squares regression analysis . The equations used for curve fitting were obtained from Young (30).

The slope m, which corresponds to $-k_2$ in the equation 7 was calculated using the following equation:

$$m = (N \Sigma x_i t_i - (\Sigma x_i)(\Sigma t_i))/ (N \Sigma x^2_i - (\Sigma x_i)^2) \qquad \text{(equation 8)}$$

where N is the total number of data points, x_i is the ratio of the bound to the total label at i^{th} data point and t_i is the dissociation time period at i^{th} data point.

The intercept b, which corresponds to ln B_o in the equation 7, was calculated using the following equation:

$$b = ((\Sigma t_i)(\Sigma x^2_i) - (\Sigma x_i t_i)(\Sigma x_i)) / (N \Sigma x^2_i - (\Sigma x_i)^2) \quad \text{(equation 9)}$$

The total variance of the data (σ) and also the variance due to both the slope (σ_m) and intercept (σ_b) were calculated using the following equations:

$$\sigma = (\Sigma (mx_i + b - t_i)^2) / N \quad \text{(equation 10)}$$

$$\sigma_m = (N\sigma) / (N \Sigma x^2_i - (\Sigma x_i)^2) \quad \text{(equation 11)}$$

$$\sigma_b = (\sigma \Sigma x_i^2) / (N \Sigma x^2_i - (\Sigma x_i)^2) \quad \text{(equation 12)}$$

The reliability of the above parameters can be known by the fit coefficient, r, calculated using the following equation:

$$r = (N \Sigma xt - \Sigma x \Sigma t) / ([N \Sigma x^2 - (\Sigma x)^2]^{1/2} [N \Sigma t^2 - (\Sigma t)^2]^{1/2}) \quad \text{(equation 13)}$$

The closer the value of r to one, the more reliable are the various parameters obtained.

The half-life period for DNA-protamine complexes was determined by using the following equation :

$$\text{Half-life } t_{1/2} = 0.693/ k_2 \quad \text{(equation 14)}$$

Biphasic kinetic data analysis

The lack of linearity of the time vs ln B_t/B_o plot could indicate more than one reaction rate was involved in the data obtained. The dissociation pattern appeared to show an initial rapid dissociation, followed by a slower dissociation over the rest of the dissociation time period. The reason for this pattern could be because of the presence of

multiple binding sites. Since the apparent nature of the dissociation was biphasic, a complex data analysis was required to calculate the rate constant for the initial dissociation reaction.

The method suggested by Moore and Pearson (31) was followed which allows the separation of the slower segment of the reaction from the faster phase. This method can be followed when the rate constants of the two phases vary in magnitude enough to separate them statistically and ample number of data points representing both the rate reactions were collected. Using the method, the both rates can be determined independently. The absolute amplitude (ΔA) was determined by subtracting the amount of DNA bound at infinite time (C_∞) from the amount of DNA bound at each time (Ct). The data point where the dissociation has reached a plateau was taken as C_∞.

$$\Delta A = C_\infty - Ct \qquad \text{(equation 15)}$$

The natural logarithm of ΔA was plotted as a function of time in minutes and the slow reaction was projected back to zero. This allowed the subtraction of the contribution of the slow reaction from the fast reaction which gave the stripped data ($\Delta\Delta A$). The natural logarithm of the stripped data $\Delta\Delta A$ was plotted as a function of time in minutes and the negative slope of the plot gave the k_2 for the fast reaction.

RESULTS

Due to the high nonspecific DNA binding observed in preliminary experiments (Table 2), the initial protocol adopted from the manufacturer was changed. Changes that helped reduce the nonspecific binding were adopted for the subsequent experiments. Table 2 gives the comparison of the percentage DNA bound to substituted and unsubstituted dynabeads. The unsubstituted dynabeads had about 25% of the total amount of labeled DNA bound at zero time of dissociation and the percentage bound increased with time. At the four hour dissociation time period, about 53% of the total amount of labeled DNA was bound to the beads. Thus, there was high nonspecific binding of the labeled DNA. No specific binding to P1 substituted dynabeads was observed. These results were in contrast to the expected results where the percentage of the total amount of the labeled DNA is maximum at zero time and it would decrease over time due to the dissociation of P1-DNA complexes assuming first order kinetics for the decay of the DNA-P1 complex.

A few experiments were conducted on the control dynabeads to reduce the nonspecific binding. Table 3 shows the effect of decreasing temperature on nonspecific DNA binding. The dynabeads and the labeled DNA were incubated at 24 ^{0}C for one hour (rather than 32 ^{0}C). Lowering the temperature reduced the nonspecific binding but it needed to be reduced further. All subsequent experiments were conducted using 24 ^{0}C during the incubation.

Table 2: Comparison of the percentage of the total amount of DNA bound to P1 substituted dynabeads to the percentage of the total amount bound to control dynabeads. P1 substituted dynabeads and the control dynabeads were incubated with the labeled DNA for one hour at 32 ^{0}C.

A: The percentage of the total amount of DNA bound to the P1 substituted dynabeads (63 nM, 40 nM DNA, 2 mg beads).

* Calculated from cpm of one tenth volume of supernatant radioactivity
** Summation of free and bound DNA cpm.

Time in hours	Cpm * Free DNA	Cpm Bound DNA	Total counts**	% bound DNA
0	40126	7963	48089	17
0.25	40090	3176	43266	7
0.5	36502	4718	41220	11
0.75	37064	4432	41496	11
1	39434	4889	44323	11
2	37500	9623	47123	20
3	27506	12294	39800	31
4	28328	23183	51511	45

B: The percentage of the total amount of DNA bound to the unsubstituted dynabeads (control).

Time in hours	Cpm Free DNA	Cpm Bound DNA	Total counts	%DNA bound
0	16588	5401	21989	25
0.25	19128	3341	22469	15
0.5	20234	4758	24992	19
0.75	19232	9082	28314	32
1	17068	10729	27797	39
2	18518	8425	26943	31
3	10802	11351	22153	51
4	15208	16922	32130	53

Table 3: Nonspecific DNA binding to dynabeads at 24 ^{0}C.

Time in hours	Cpm Free DNA	Cpm Bound DNA	Total counts	% bound DNA
0	57880	9488	67368	14
0.25	49900	18373	68273	27
0.5	60740	17994	78734	23
0.75	53260	10570	63830	17
1	50920	17052	67972	25
2	52960	16881	69841	24
3	78260	10776	89036	12
4	67410	11604	79014	15

Note: The percentage of the total amount of DNA bound to the control dynabeads incubated with 12 pmol of the labeled DNA in 150 micro liters at 24 ^{0}C.

Table 4: The effect of competitor, unlabeled DNA on nonspecific binding.

A: The percentage of the total amount of labeled DNA bound to unsubstituted dynabeads using a specific activity of 8.1×10^5 cpm / 100 pmol DNA).

Time in hours	Cpm Free DNA	Cpm Bound DNA	Total counts	% bound DNA
0	43000	4074	47074	9
0.25	44055	5090	49145	10
0.5	39620	6908	46528	15
0.75	43740	6386	50126	13
1	40715	7394	48109	15
1.5	36010	6809	42819	16
2	44560	7999	52559	15

B: The percentage of the total amount of labeled DNA bound to unsubstituted dynabeads using a specific activity of 3.3×10^5 cpm / 100 pmol DNA).

Time in hours	Cpm Free DNA	Cpm Bound DNA	Total counts	% bound DNA
0	33145	7249	40394	18
0.25	40670	4812	45482	11
0.75	35560	4626	40186	12
1	35130	4946	40076	12
1.5	32570	6079	38649	16
2	37310	6221	43531	14

The effect of an excess of competitor, unlabeled DNA, in the reduction of the nonspecific binding is given in Table 4. The results showed that the percentage of the total amount of DNA bound to the control was similar for a small range of specificity activities, and the nonspecific binding was still high. Table 5 shows the effect of using 0.1% Bovine Serum Albumin (BSA) during the preparation of the dynabeads as suggested by the manufacturer. The results showed that the nonspecific binding was very high, about 47% on an average. This experiment eliminated the potential use of BSA during the preparation of dynabeads.

The effect of different NaCl concentrations in the dissociation buffer was also examined (Table 6). Four different concentrations of NaCl (0, 0.05, 0.1, and 0.5 M) were used. For 0 M NaCl concentration, the nonspecific binding was very high at zero time but reduced after one hour dissociation time period. The nonspecific binding was high for all the concentrations of NaCl used in the dissociation buffer.

Table 7 shows the results obtained by using a preservative, 0.01% sodium azide, in all solutions. The use of sodium azide would eliminate the bacterial growth in the dynabeads. The average nonspecific binding was about 7% which was the lowest nonspecific binding compared to previous experiments. In subsequent experiments, 0.01% sodium azide was added to all buffers.

The final conditions used for the dissociation experiments were, 0.01% sodium azide in all buffers, 24 ^{0}C incubation temperature and 0.1 M NaCl along with 50 mM HEPES in the dissociation buffer.

Table 5: Effect of using 0.1% Bovine Serum Albumin on nonspecific binding. A and B show the results from two preparations of the dynabeads.

A:

Time in hours	Cpm Free DNA	Cpm Bound DNA	Total counts	% bound DNA
0	15380	10346	25726	40
0.5	16110	11193	27303	41
1	17260	13870	31130	45
1.5	18080	15370	33450	46
2	11700	12401	24101	51
24	13500	16969	30469	56

B:

Time in hours	Cpm Free DNA	Cpm Bound DNA	Total counts	% bound DNA
0	15350	11647	26997	43
0.5	15330	12954	28284	46
1	16080	14227	30307	47
1.5	17130	16148	33278	49
2	16340	14798	31138	48
24	13800	15493	29293	53

Table 6: Effect of using different concentrations of NaCl in the dissociation buffer on nonspecific binding.

A: Use of 50 mM HEPES as the dissociation buffer.

Time in hours	Cpm Free DNA	Cpm Bound DNA	Total counts	% bound DNA
0	13240	18711	31951	59
0	13360	20897	34257	61
0.5	28650	11061	39711	28
0.5	28950	12229	41179	30
1	32120	8659	40779	21
1	32390	9084	41474	22
2	39770	5196	44966	12
2	37610	6820	44430	15

B: Use of 50 mM HEPES in 50 mM NaCl as the dissociation buffer.

Time in hours	Cpm Free DNA	Cpm Bound DNA	Total counts	% bound DNA
0	23200	7709	30909	25
0	26250	8307	34557	24
0.5	25640	8917	34557	26
0.5	25180	9732	34912	28
1	23340	8882	32222	28
1	22940	9279	32219	29
2	25670	10094	35764	28
2	25020	10269	35289	29

Table 6: Continued

C: Use of 50 mM HEPES in 100 mM NaCl as the dissociation buffer.

Time in hours	Cpm Free DNA	Cpm Bound DNA	Total counts	% bound DNA
0	17540	7545	25085	30
0	17690	8285	25975	32
0.5	19500	10616	30116	35
0.5	18720	11308	30028	38
1	19800	10328	30128	34
1	19160	12391	31551	39
2	20960	12140	33100	37
2	18950	12129	31079	39

D: Use of 50 mM HEPES in 500 mM NaCl as the dissociation buffer.

Time in hours	Cpm Free DNA	Cpm Bound DNA	Total counts	% bound DNA
0	15230	7334	22564	33
0	14290	6379	20669	31
0.5	14180	8963	23143	39
0.5	13340	9965	23305	43
1	13730	9957	23687	42
1	13980	10563	24543	43
2	14870	11257	26127	43
2	14550	10800	25350	43

Table 7: Effect of using 0.01% sodium azide in all buffers on nonspecific binding. Results from two preparations of the dynabeads are shown.

A:

Time in hours	Cpm Free DNA	Cpm Bound DNA	Total counts	% bound DNA
0	32350	1877	34227	5
1	31930	2693	34623	8
2	33390	1502	34892	4
4	31890	2613	34503	8
24	31880	3048	34928	9

B:

Time in hours	Cpm Free DNA	Cpm Bound DNA	Total counts	% bound DNA
0	39900	1774	41674	4
1	39190	2802	41992	7
2	37570	4088	41658	10
4	37890	3974	41864	9
24	39840	2456	42296	6

Dissociation of labeled DNA from P1 substituted dynabeads

Two different dissociation experiments using the same batch of P1 substituted dynabeads were conducted to determine the dissociation rate constant of P1-DNA complexes. Figure 7 shows the dissociation pattern for the P1-DNA complexes. Although there is scatter in the data, the dissociation rate constant values calculated from the two experiments are the same within experiment error, $3.3 \pm 0.55 \times 10^{-5} s^{-1}$ and $3.3 \pm 1.0 \times 10^{-5} s^{-1}$(Figure 7B and 7D, respectively).

Dissociation of labeled DNA from P2 substituted dynabeads

Experiments were performed to determine the dissociation rate constant for hamster protamine P2-DNA complexes. Two experiments using different preparations of dynabeads were conducted to demonstrate the percentage of labeled DNA bound to the P2 substituted dynabeads (Table 9). The results showed that there was less percentage of the labeled DNA bound to the P2-dynabeads at zero time, which was not sufficient to perform the dissociation protocol. When the concentration of P2 was increased two fold an increase in the percentage of labeled DNA bound to the P2 substituted dynabeads at zero time (19%) was observed. Thus the amount of P2 added for substitution on dynabeads was an important parameter affecting the total % of DNA bound. Figure 8 shows the dissociation pattern for the P2-DNA complexes with two fold increase in the P2 concentration. The dissociation rate constant calculated from Figure 8B was $7.5 \times 10^{-5}/s^{1}$. Another experiment was conducted using a different batch of dynabeads to determine the

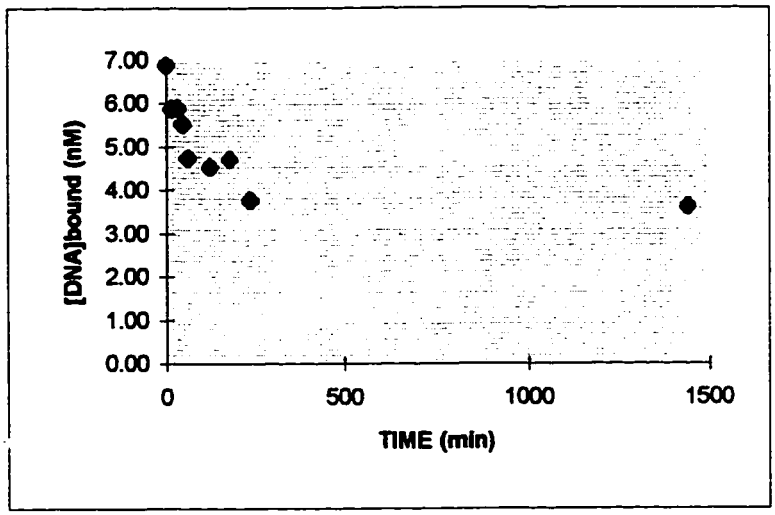

A: The concentration of specifically bound DNA (nM) to the P1 substituted dynabeads shown as a function of time.

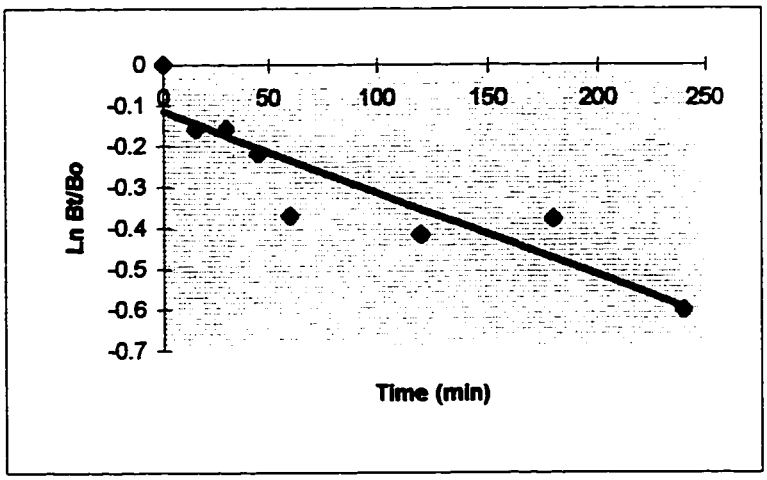

B: The natural logarithm of the ratio of bound DNA at any time to that bound at zero time shown as a function of time. The line represents the linear least squares regression for the dissociation of DNA from P1 substituted dynabeads.

$y = -0.002x - 0.1151$, $R^2 = 0.8192$

Figure 7: Determination of the rate of dissociation of the DNA from P1 substituted dynabeads.
(All samples contained 63 nM P1 and 27.5 nM DNA).

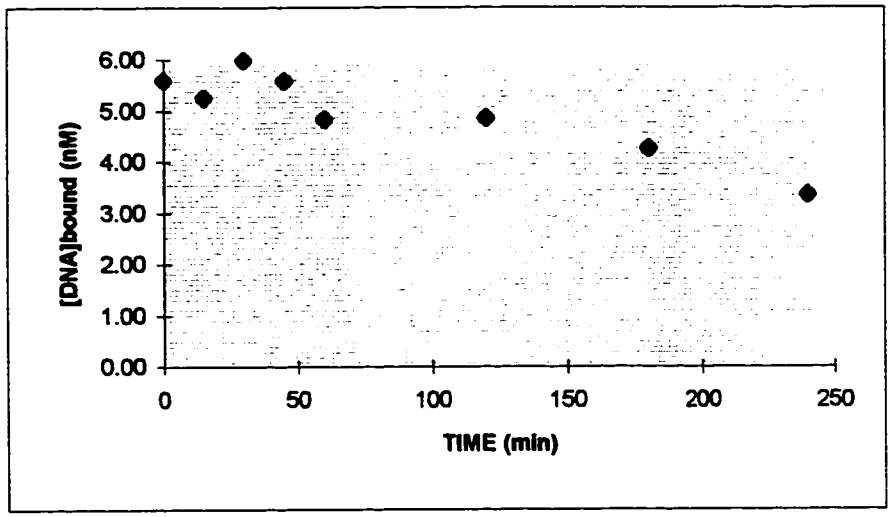

C: The concentration of specifically bound DNA (nM) to the P1 substituted dynabeads shown as a function of time.

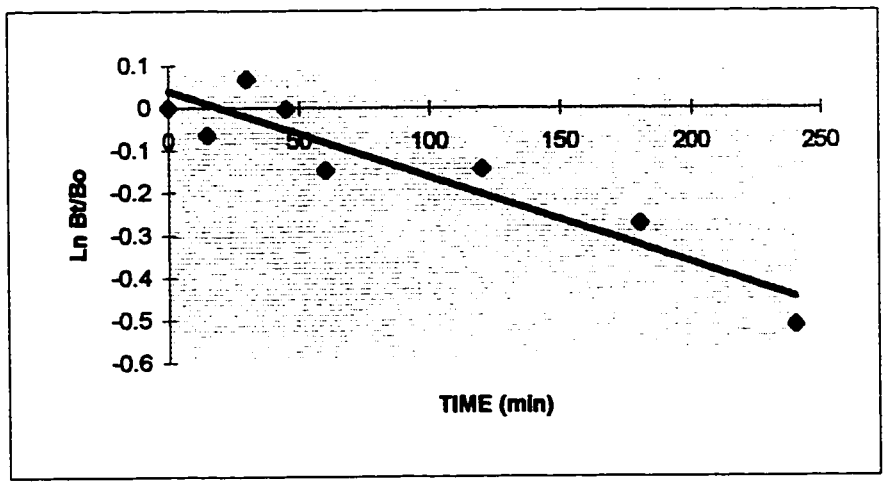

D: The natural logarithm of the ratio of bound DNA at any time to that bound at zero time shown as a function of time. The line represents the linear least squares regression for the dissociation of DNA from P1 substituted dynabeads.

$y = -0.002x + 0.04$, $R^2 = 0.8677$

Figure 7: Continued

(The magnitude of the error bars are contained within the symbols of the figure.)

Table 8: The percentage of the total amount of labeled DNA bound to unsubstituted dynabeads.

Time in hours	Cpm for Free DNA	Cpm for Bound DNA	Total counts	% bound DNA
0	106680	6136	112816	5
0.25	103120	8519	111639	8
0.5	100150	10813	110963	10
0.75	99380	11464	110844	10
1	95530	11968	107498	11
2	99310	10322	109632	9
3	99900	12327	112227	11
4	100440	7278	107718	7
24	97800	7659	105459	7

Note: An average of 8% binding observed from unsubstituted dynabeads was subtracted from the labeled DNA bound to P1 substituted dynabeads to yield specific binding in Figure 7.

.

Table 9: The percentage of the total amount of labeled DNA bound to the P2 substituted dynabeads.
A and B represent the results from the dissociation separate of two preparations of dynabeads are shown.

A:

Time in hours	Cpm Free DNA	Cpm Bound DNA	Total counts	% bound DNA
0	49020	1521	50541	3
0.25	46530	2835	49365	6
0.5	47490	2473	49963	5
0.75	50340	2408	52748	5
1	39540	4524	44064	11
2	39380	38210	77590	97
3	35920	11783	47703	33
4	35150	8018	43168	23
24	37410	10089	47499	27

B:

Time in hours	Cpm for Free DNA	Cpm for Bound DNA	Total counts	% bound DNA
0	48980	1944	50924	4
0.25	47710	2773	50483	6
0.5	46860	3557	50417	8
0.75	49050	1398	50448	3
1	40610	4320	44930	11
2	43610	5405	49015	12
3	38660	9755	48415	25
4	31500	12382	43882	39
24	37170	10460	47630	28

Note: (All samples contained 63 nM P2 and 22.5 nM DNA).

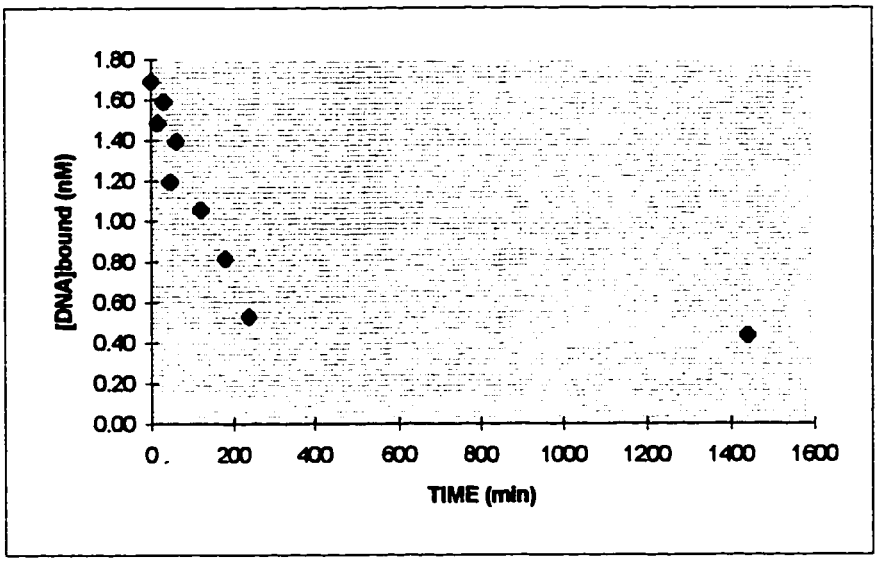

A: The concentration of specifically bound DNA (nM) to the P2 substituted dynabeads shown as a function of time.

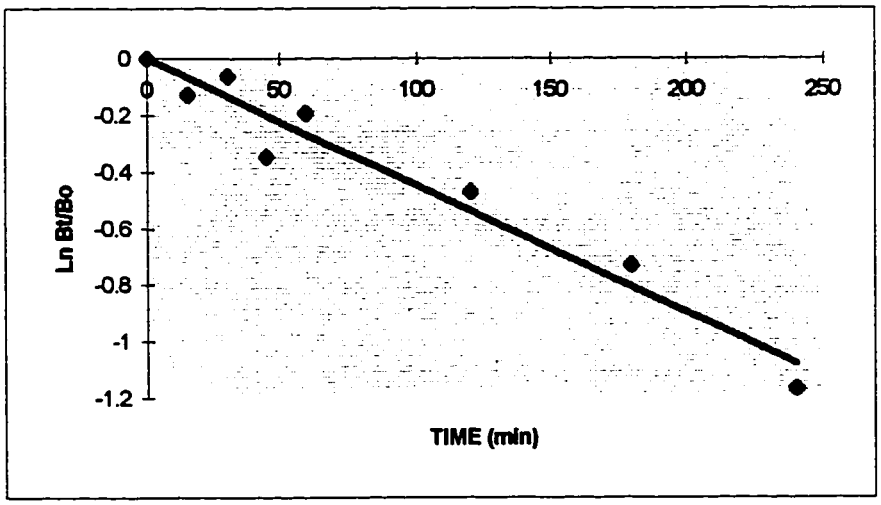

B: The natural logarithm of the ratio of bound DNA at any time to that bound at zero time shown as a function of time. The line represents the linear least squares regression for the dissociation of DNA from P2 substituted dynabeads.
$y = -0.0045x - 0.0007$, $R^2 = 0.9503$

Figure 8: Determination of the rate of dissociation of the DNA from P2 substituted dynabeads.
(All samples contained 126 nM P2 and 22.5 nM DNA).

determine the dissociation rate constant for P2-DNA complexes. In the above experiment about 10 fold concentration of P2 was required to obtain reasonable percentage of labeled DNA bound to P2 substituted dynabeads at zero time (18.5%). Figure 9 shows the dissociation pattern for the P2-DNA complexes for the above experiment. The dissociation rate constant calculated from Figure 9B was 7.5×10^{-5} s^{-1}. Thus the k_2 value determined from both the experiments was the same within experiment error though different concentrations of P2 and different batches of dynabeads were used in each experiment.

Dissociation of labeled DNA from P2 highly substituted dynabeads

Two experiments were conducted to determine the dissociation of labeled DNA from highly substituted dynabeads. For these experiments a single preparation of batch B dynabeads substituted with fivefold concentration of P2 were used. Figures 10 and 11 show the dissociation pattern for the labeled DNA from highly substituted P2-dynabeads. The dissociation rate constants calculated from Figures 10B and 11B were 5.9×10^{-5} s^{-1} and 7×10^{-5} s^{-1} respectively. The correlation coefficients for the least squares fit through the data was poor in both the above figures. The magnitude of the error bars are contained within the symbols of the figures. The dissociation pattern showed initial rapid dissociation followed by a slower dissociation over the rest of the dissociation time period. Since the apparent nature of the dissociation was biphasic, additional data analysis was required to calculate the rate constant for the initial dissociation reaction. The method

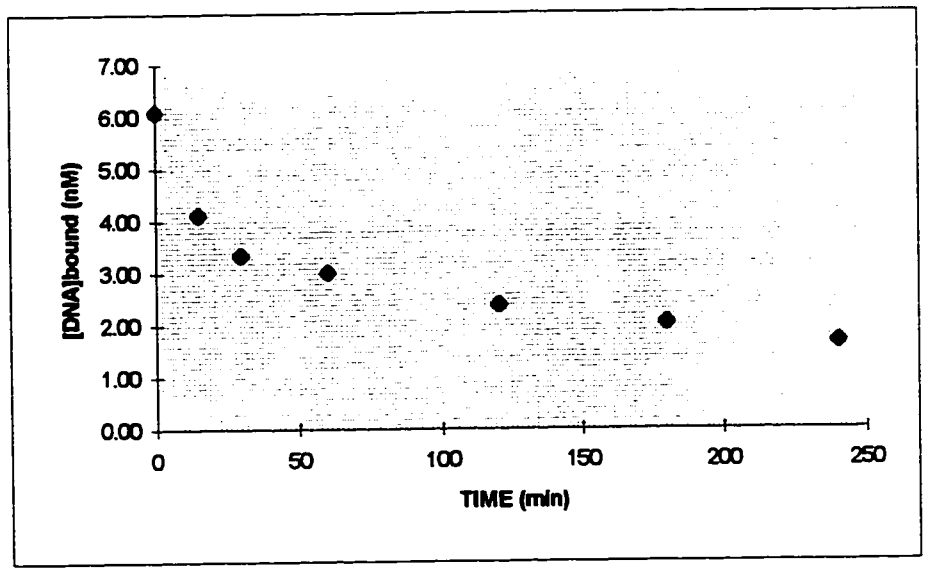

A: The concentration of specifically bound DNA (nM) to the P2 substituted dynabeads shown as a function of time.

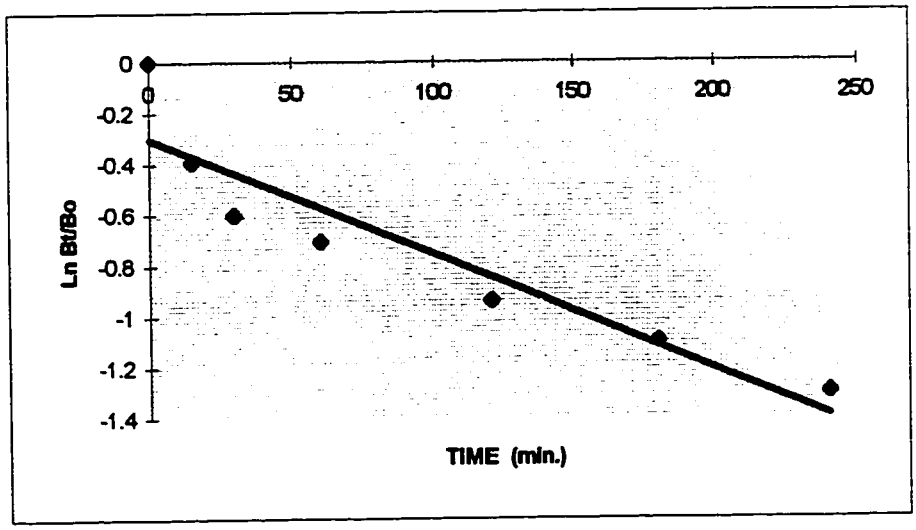

B: The natural logarithm of the ratio of bound DNA at any time to that bound at zero time shown as a function of time. The line represents the linear least squares regression for the dissociation of DNA from P2 substituted dynabeads.
$y = -0.0045x - 0.3027$, $R^2 = 0.8696$

Figure 9: Determination of the rate of dissociation of the DNA from P2 substituted dynabeads.
(All samples contained 630 nM P2 and 42 nM DNA).

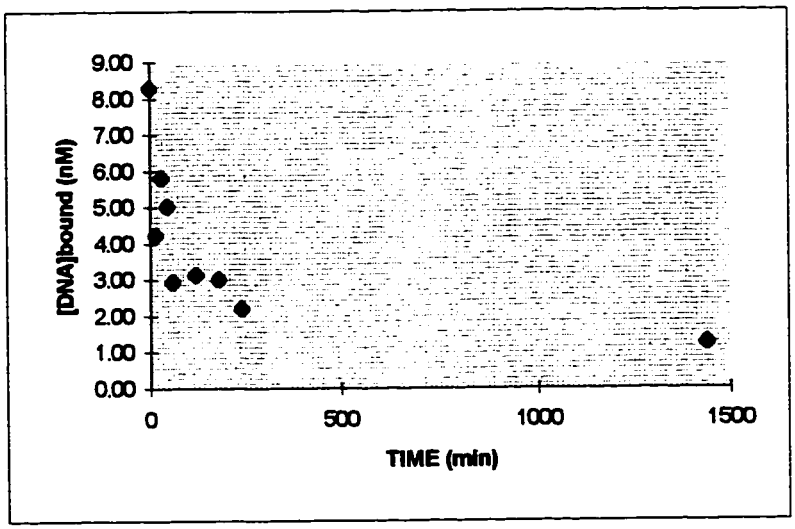

A: The concentration of specifically bound DNA (nM) to the P2 substituted dynabeads shown as a function of time.

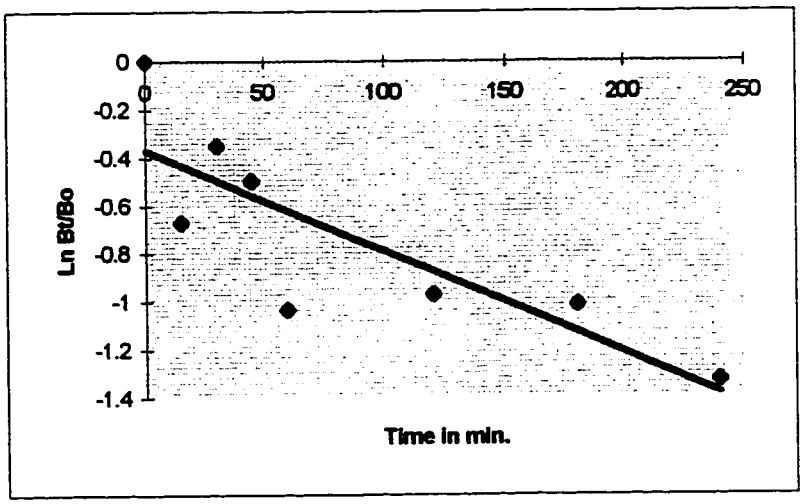

B: The natural logarithm of the ratio of bound DNA at any time to that bound at zero time shown as a function of time. The line represents the linear least squares regression for the dissociation of DNA from P2 substituted dynabeads.

$y = -0.0042x - 0.3719$, $R^2 = 0.687$

Figure 10: Determination of the rate of dissociation of the DNA from P2 highly substituted dynabeads.
(All samples contained 315 nM P2 and 22.5 nM DNA).

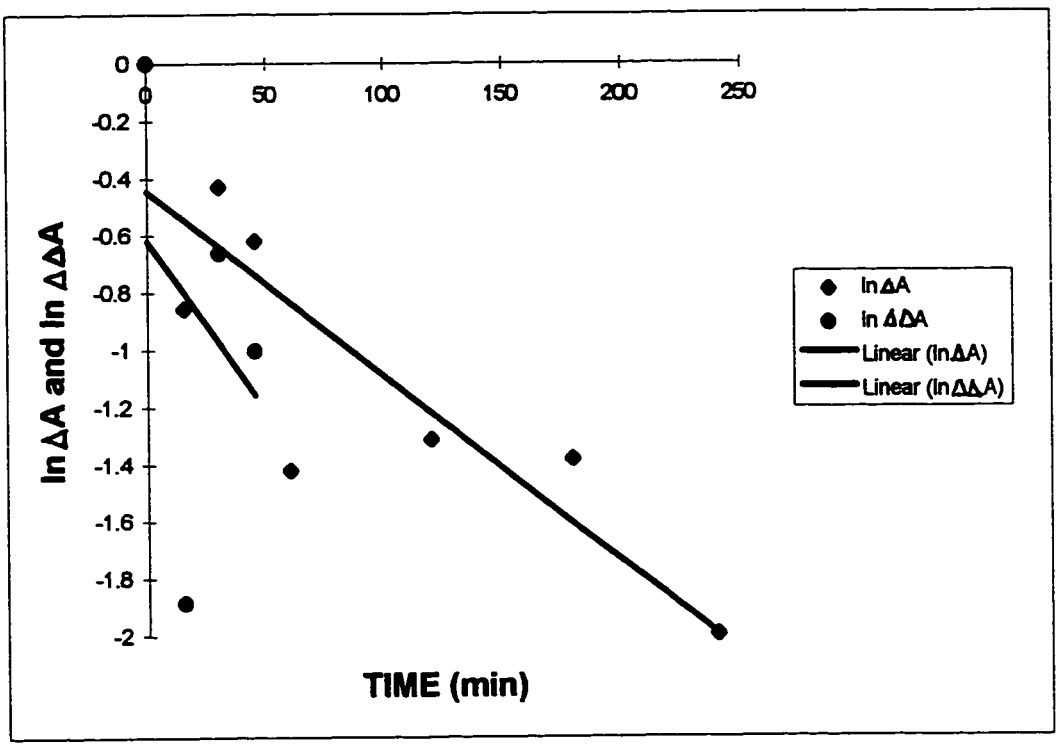

Figure 10C: The natural logarithms of absolute amplitude (ΔA) and the stripped data ($\Delta\Delta A$) are plotted as a function of time in minutes. Linear lines, ln ΔA and ln $\Delta\Delta A$ are the least square lines for the slow and fast reactions respectively.

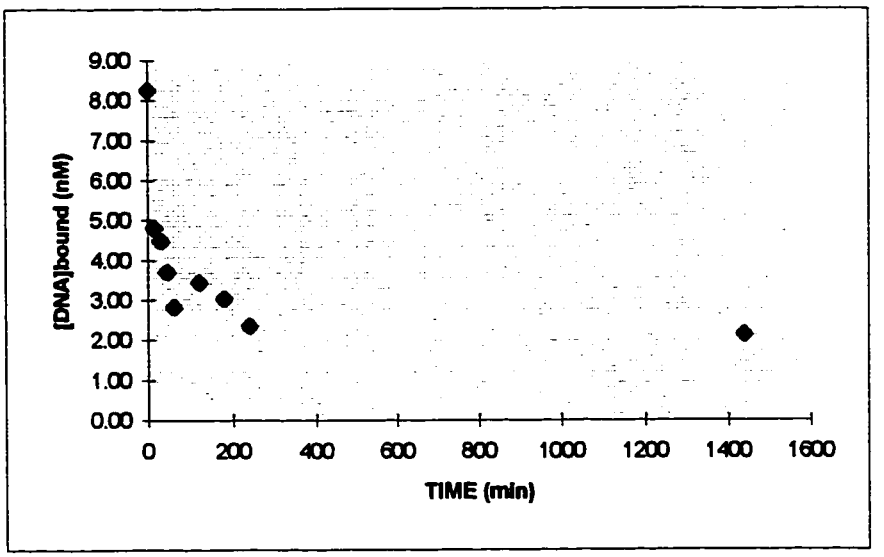

A: The concentration of specifically bound DNA (nM) to the P2 substituted dynabeads shown as a function of time.

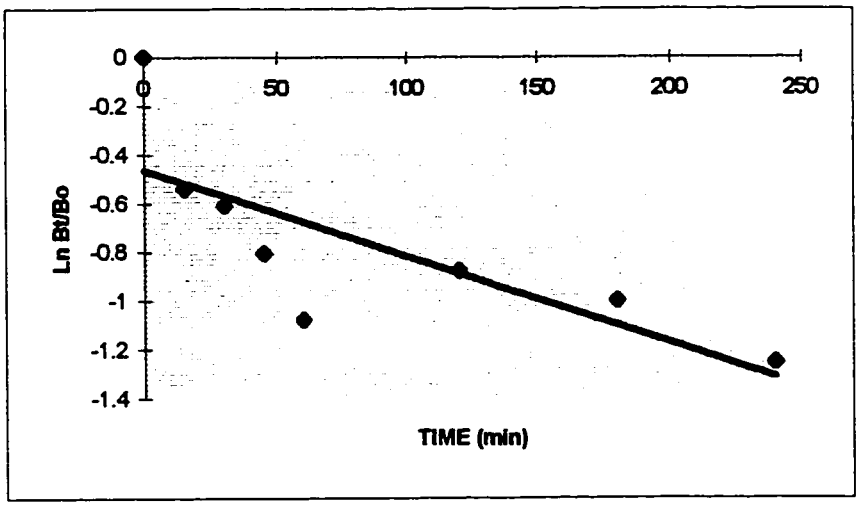

B: The natural logarithm of the ratio of bound DNA at any time to that bound at zero time shown as a function of time. The line represents the linear least squares regression for the dissociation of DNA from P2 substituted dynabeads.

$y = -0.0035x - 0.466$, $R^2 = 0.6022$

Figure 11: Determination of the rate of dissociation of the DNA from P2 highly substituted dynabeads.
(All samples contained 315 nM P2 and 22.5 nM DNA).

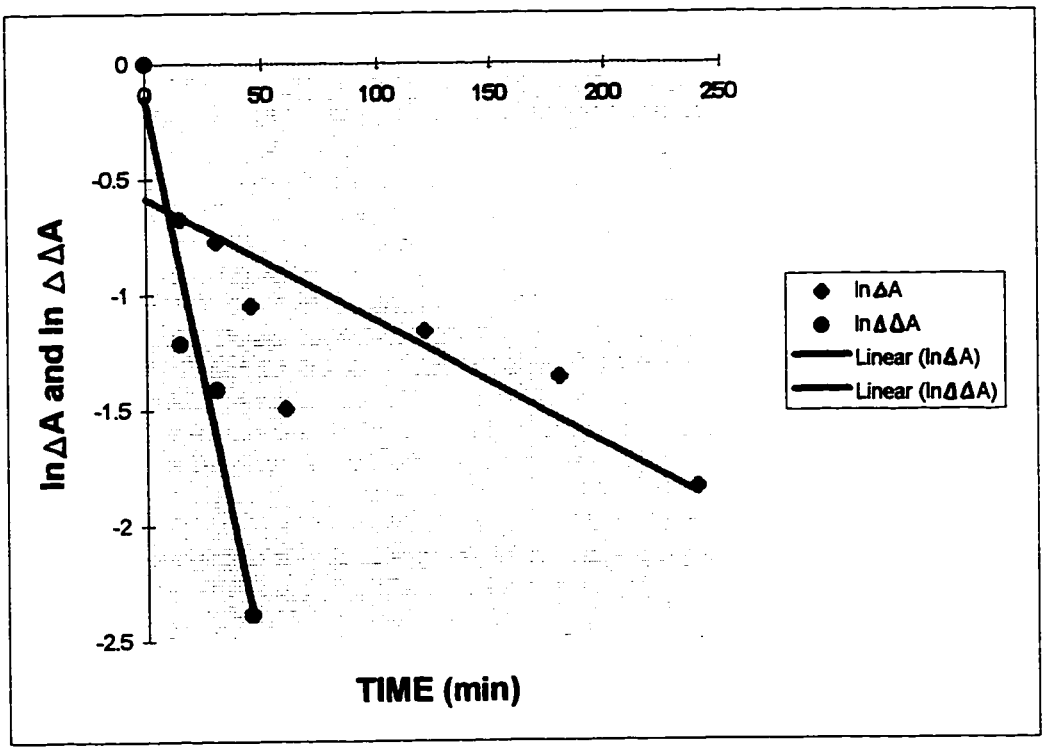

Figure 11C: The natural logarithms of absolute amplitude (ΔA) and the stripped data (ΔΔA) are plotted as a function of time in minutes. Linear lines, ln ΔA and ln ΔΔA are the least square lines for the slow and fast reactions respectively.

Table 10: The percentage of the total amount of labeled DNA bound to unsubstituted dynabeads.

Time in hours	Cpm Free DNA	Cpm Bound DNA	Total counts	% bound DNA
0	42530	2736	45266	6
0.25	42190	3481	45671	8
0.5	38980	5020	44000	11
0.75	42320	3630	45950	8
1	39442	3562	43004	8
2	40560	4632	45192	10
3	37850	4318	42168	10
4	40690	4523	45213	10
24	38560	4124	42684	10

Note: An average of 9% binding observed from unsubstituted dynabeads was subtracted from the labeled DNA bound to P2 substituted dynabeads to yield specific binding in Figure 8, 10 and 11.

segment of the reaction from the faster phase. This method can be followed when the rate constants of the two phases vary in magnitude enough to separate them statistically. So the rates of both the phases can be determined independently.

The natural logarithms of absolute amplitude and the stripped data plotted as a function of time in minutes for the above experiments are shown in Figures 10C and 11C respectively. The k_2 values obtained for the slow and fast reaction from Figure 10C are $1.1 \times 10^{-4}\ s^{-1}$ and $2 \times 10^{-4}\ s^{-1}$ respectively. The k_2 values obtained for the slow and fast reaction from Figure 11C are $8.9 \times 10^{-5}\ s^{-1}$ and $8.2 \times 10^{-4}\ s^{-1}$, respectively.

Dissociation of labeled DNA from P2 substituted thiol activated sepharose resin

The dissociation rate constant for the P2-DNA complexes was also determined using thiol activated sepharose resin as a solid substrate. This experiment is the positive control for the previous experiments involving P2 and dynabeads. Figure 12 shows the dissociation pattern for the P2-DNA complexes using thiol activated sepharose resin The dissociation rate constant calculated from Figure 6B was $3.6 \times 10^{-5}\ s^{-1}$. Thus the k_2 values determined using dynabeads and thiol activated sepharose resin are in the same magnitude ($10^{-5}\ s^{-1}$).

The summary of all the dissociation experiments conducted was given in Tables 11, 12 and 13. Table 11 gives the comparison of the k_2 values determined for P1-DNA complexes from two experiments. Table 12 gives the comparison of the k_2 values determined for P2-DNA complexes from five experiments, four with P2 substituted

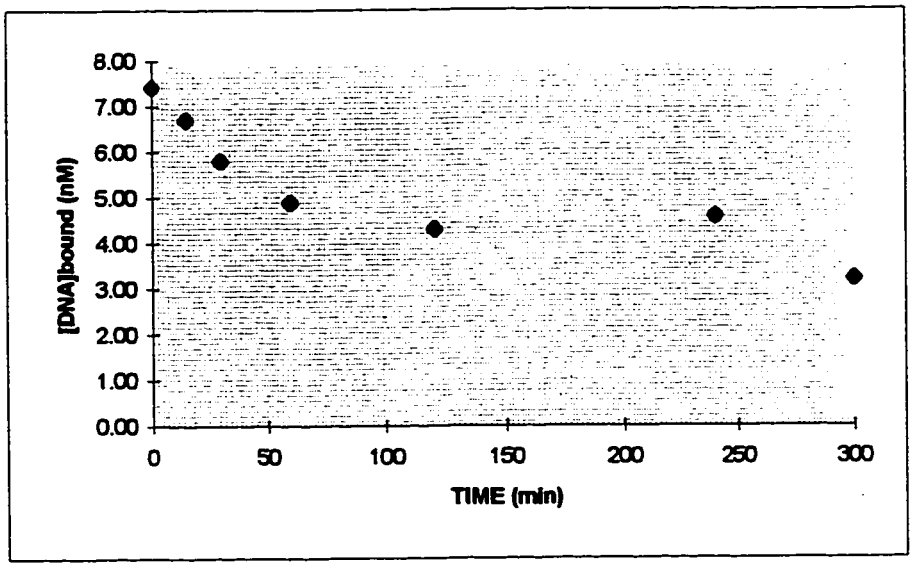

A: The concentration of specifically bound DNA (nM) to the P2 substituted sepharose resin shown as a function of time.

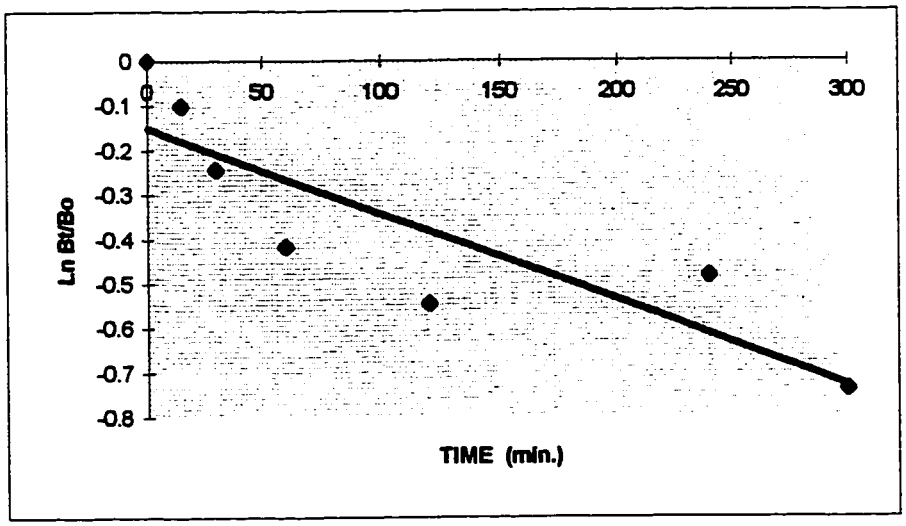

B: The natural logarithm of the ratio of bound DNA at any time to that bound at zero time shown as a function of time. The line represents the linear least squares regression for the dissociation of DNA from P2 substituted dynabeads.

$y = -0.0019x - 0.1505$, $R^2 = 0.7631$

Figure 12: Determination of the rate of dissociation of the DNA from P2 substituted thiol activated sepharose resin.
(All samples contained 315 nM P2 and 42 nM DNA).

Table 11: The dissociation rate constant (k_2) values obtained for P1-DNA complexes in two experiments are compared.

Experiment	Dynabead sample	nM P1	nM DNA	k_2 (x 10 +5)s^{-1}	$t_{1/2}$ (min)
1	A	63	27.5	3.37	342
2	A	63	27.5	3.33	347

Table 12: The dissociation rate constant (k_2) values obtained for P2-DNA complexes in five experiments are compared.

Experiment	Dynabead sample	nM P2	nM DNA	k2 (x 10 +5)s^{-1}	$t_{1/2}$ (min)
1	B	126	22.5	7.5	154
2	B	315	22.5	5.9	196
3	B	315	22.5	7	165
4	D	630	42	7.5	154
5	Sepharose resin	315	42	3.6	320

Table 13: The % DNA bound to the P2 substituted dynabeads at zero time obtained for P2-DNA complexes in eight experiments are compared.

Experiment	Dynabead sample	nM P2	nM DNA	% DNA bound at zero time	k_2 (x 10 +5)s^{-1}
1	B	126	22.5	19	7.5
2	B	315	22.5	70	5.9
3	B	315	22.5	69	7
4	D	630	42	18.5	7.5
5	C	126	66.5	4.6	
6	C	315	66.5	2.5	
7	D	126	75	4.2	
8	D	315	75	2.8	

determined for P2-DNA complexes from five experiments, four with P2 substituted dynabeads and one with P2 substituted on thiol activated sepharose resin. Table 13 gives the comparison of the % DNA bound to the P2 substituted dynabeads at zero time. The k_2 values were given for the first four experiments since the dissociation protocol was conducted in those experiments. But for the last four experiments, the k_2 value was not determined because the % DNA bound to the P2 substituted dynabeads at zero time was very low.

Effect of the concentration of NaCl on the dissociation of protamine-DNA complex

The effect of the concentration of NaCl on the dissociation of the highly substituted dynabeads was performed by rinsing the highly substituted dynabeads with increasing concentrations of NaCl. A portion of the supernatant was taken after each rinse and counted in order to determine the release of DNA with increasing NaCl concentration. Figure 13 shows the cumulative percentage of labeled DNA freed as a function of the NaCl concentration used in the rinse buffer.

Rinsing the dynabeads with 0.1 M NaCl showed substantial dissociation. A big increase in the dissociation was observed between 0.1 M and 0.4 M NaCl. At 1.0 M NaCl, about 20% of the DNA was still bound to the dynabeads. The nonspecific binding for the control was about 6% throughout the process. Therefore about 14% of the labeled DNA was irreversibly bound to the P2 even after rinsing with high ionic strength buffer.

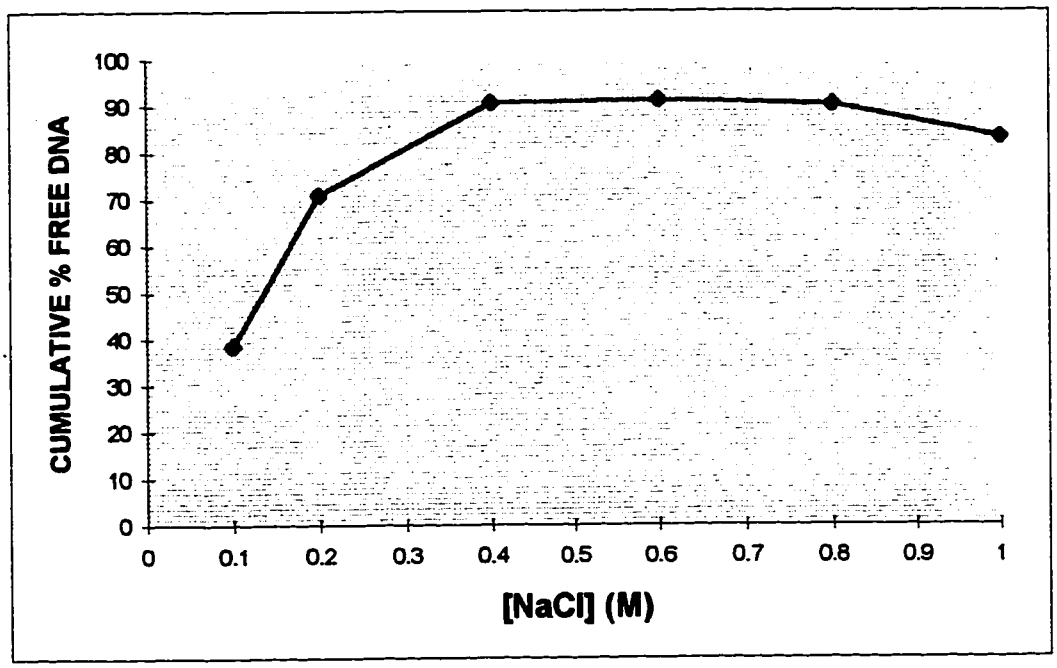

Figure 13: The cumulative percent of the labeled free DNA is plotted as a function of the concentration of NaCl. The indicated concentration of NaCl on the x-axis was added to 50mM HEPES. 1 ml solution of each of these rinse the dynabeads. Each point is an average of duplicate samples.

DISCUSSION

Suitability of tosylactivated dynabeads to study protamine-DNA interactions

The first objective of the study was to establish the dynabead system as a solid substrate method to examine the kinetics of protamine-DNA interactions. Bull protamine P1 and hamster protamine P2 were immobilized on dynabeads in the present study. The immobilization of a protein on dynabeads takes place through the replacement of the tosyl group by the primary amine group of the N terminal amino acid or by the sulfhydral group of a cysteine residue at pH 9.5 (information provided by the manufacturer of dynabeads).

One of the most important requirements for choice of solid substrates, is a low background or nonspecific binding of the radiolabeled DNA. The results given in Table 2 show that at 32 ^{0}C and under the other conditions specified, the nonspecific binding varied from about 7 to 53% over a period of 0 to 4 hours. The nonspecific binding increased with time. This was very high compared to the 3 to 5% nonspecific binding associated with thiol activated (24) and 1-1'- Carbonyldiimadazole activated (32) sepharose resins that have been used for protamine-DNA dissociation experiments.

A decrease in the temperature of incubation of dynabeads with labeled DNA from 32 to 24 ^{0}C reduced the nonspecific binding to about 14 to 25% as shown in Table 3. All the later experiments were conducted at 24 ^{0}C since there seemed to be a significant reduction in nonspecific binding. But 14 to 25% nonspecific binding was still too high to conduct dissociation experiments. Changes in the specific activity of labeled DNA (Table

4) did not reduce the nonspecific binding. Addition of 0.1% BSA didn't help reduce the nonspecific binding as shown in Table 5. The concentration of NaCl was varied in the dissociation buffer as shown in Table 6, but none of the compositions of the dissociation buffer used reduced the nonspecific binding. The results in Table 7 show that the use of 0.01% sodium azide in the buffers significantly reduced the nonspecific binding to an average of about 7%. It is known that sodium azide eliminates the growth of bacteria. The nonspecific binding previously observed could be due to bacterial growth and contamination of the dynabeads at room temperature. In subsequent experiments, 0.01% sodium azide was added to all the buffers. The parameters like the addition of BSA which did not reduce the nonspecific binding were not reevaluated in the presence of 0.01% sodium azide. Thus, it is not known what effect the above parameters might have on the nonspecific binding in the presence of sodium azide.

One important requirement for the solid substrate is that it should be easily activated. In the present case, preactivated dynabeads (tosylactivated dynabeads) were used. The reproducibility of the extent of substitution of tosyl group on dynabeads was not tested in the present study. Another important requirement for the solid substrate is that it should demonstrate reproducible and controllable immobilization or binding of the reactant (protamine in the present study). An indirect measure of P1 or P2 substitution is a measurement of DNA binding. Thiol activated sepharose resin showed an increase in the binding of DNA to the P1 substituted resin with an increase in the input of P1 (24). This trend was not observed in case of P2 substituted dynabeads. Table 13 shows the

percentage of the labeled DNA bound to P2 substituted dynabeads at zero time in eight experiments. Different batches of M-280 tosylactivated dynabeads were used for different experiments shown in Table 13. The concentration of P2 used in the experiments was different and it varied from 126 to 630 nM. In the first four experiments, the percentage of the labeled DNA bound to the P2 substituted dynabeads varied from 19 to 70% which allowed a determination of dissociation kinetics. But in the last four experiments, the percentage of the labeled DNA bound to the P2 substituted dynabeads is less than 5%, which is in the range of nonspecific binding. Dissociation experiments were not conducted for those samples since the percentage binding at zero time was so low.

The poor binding of the labeled DNA to some P2 substituted dynabeads could be due to the poor substitution of P2 on the dynabeads or the poor binding of labeled DNA to the P2 substituted dynabeads. The extent of substitution of P2 on dynabeads can be determined by radioactively labeling the P2 molecules. In the present experiment, the extent of substitution of P2 molecules on dynabeads was not measured. Future work could use radioactively labeled P2 molecules to determine the extent of P2 substitution on dynabeads.

The poor substitution of P2 on dynabeads could be due to some characteristics of dynabeads or protamines. The dynabeads used for this study were M-280 tosylactivated dynabeads. These beads have been used in various experiments for protein purification, cell separation and immunoassays (25, 26). No references were found in the literature discussing the reproducibility of substitution of proteins on tosylactivated dynabeads or

involving tosylactivated dynabeads in studies of kinetics of protein-DNA binding interactions. The reason for poor reproducibility of the DNA binding could be due to the differences in the stability and reactivity of the tosylactivated groups in different samples of dynabeads. The activation of the required functional group on the beads before use in the laboratory would usually give better reproducible results rather than buying the preactivated beads from the manufacturer (L. Silberstein, personal communication). The reactivity and stability of the preactivated groups might change over a period of time leading to inconsistent results.

Balhorn (3) proposed that the secondary structure of bull protamine P1, is dependent on the extent of oxidation. In bull protamine P1, there are seven cysteine residues, as shown in Figure 2. Three cysteine residues are available for replacing the tosyl group on the dynabeads (the other four cysteines are involved in intramolecular disulfide linkages in the oxidized state) (3). The three cysteine residues are present in different locations of the P1 molecule, one in the N-terminal domain and two in the central DNA binding domain. There is a primary amine group on the N-terminal amino acid which also replaces the tosyl groups on the dynabeads. So theoretically the immobilization of P1 on dynabeads can take place at least through four different attachments (or configurations), each with its own DNA binding characteristics. The attachments involving the cysteine residues present in the central domain of the P1 molecules may be inaccessible for the binding of the DNA . If one assumes that all the four attachments

of the P1 molecules added would be attached to the dynabeads in a configuration suitable for the binding of DNA.

There are a minimum of six cysteine residues present in hamster P2 molecule (three amino acids are not identified yet) (1). There are no references found in the literature on the oxidation state of cysteine residues of hamster P2. So it is unknown how many of the six cysteine residues are available for attachment with dynabeads. It is not possible to predict the probability of the P2 molecules added that would be attached to the dynabeads in a configuration suitable for the binding of DNA.

Previous studies (32) showed that there was a low binding of the labeled DNA to the P1 substituted resin when the the P1 molecules were present as aggregates. The aggregates could result in uneven substitution of P1 on dynabeads or could lower the effective concentration of protamine solution. In the present study, freshly prepared solutions of P1 were used, to avoid the problem of aggregation of the protamines. The hamster P2 used was stored in solution throughout out the span of the experiments conducted, which was about 12 months, and was stored at -20 ^{0}C. No aggregation of the P2 molecules was observed as determined by the lack of an increased UV absorbance at 320 nm. But the P2 might be undergoing some conformational changes in solution over time that may be responsible for the low binding of the labeled DNA to the P2 substituted dynabeads.

Another reason for low binding could be the lack of spacer region between the protamine molecules and the surface of the dynabeads. Steric hindrance for the

approaching DNA might result in low binding of DNA. The use of an extended linker arm on the dynabeads with a suitable functional group at the terminus will help elucidate the role of steric hinderance and increase binding of DNA to the protamine substituted dynabeads.

Dissociation rate constant of DNA-P1 complexes

The dissociation rate constant for the bull protamine P1 and DNA complexes was determined in two experiments using tosylactivated dynabeads as a solid substrate. The values for the dissociation rate constant obtained were $3.37 \times 10^{-5} \pm 0.5 \times 10^{-5}$ and $3.33 \times 10^{-5} \pm 1.0 \times 10^{-5}$ s^{-1}. The respective half-life periods for the complexes were 342 minutes and 347 minutes. The dissociation rate constant determined using thiol activated sepharose resin was $8.9 \times 10^{-5} \pm 4.4 \times 10^{-5}$ s^{-1} (24). The dissociation rate constant obtained by using tosylactivated dynabeads as a solid substrate is in the same range as that obtained using thiol activated sepharose resin as the solid substrate (24).
These experiments were used as a control to check the suitability and reliability of tosylactivated dynabeads as a solid substrate to determine the dissociation rate constant of protamine P2-DNA interactions.

Dissociation rate constant of DNA-P2 complexes

The dissociation rate constant and half life period determined for hamster protamine P2 and DNA complexes are given in Table 12. The k_2 value obtained was 6.7 x

$10^{-5} \pm 0.8 \times 10^{-5}$ s^{-1}. With those P2 substituted dynabeads that yielded at least 18% bound DNA at zero time, the dissociation experiments were carried out, and the k_2 determined was within the range. The dissociation rate constant and half life period for P2-DNA complexes was also determined using thiol activated sepharose resin as a solid substrate. The dissociation rate constant calculated was 3.6×10^{-5} s^{-1}. This value was in the same range as that determined using dynabeads. So the experiment using sepharose resin works as a positive control for the experiments conducted using dynabeads. Additionally, it appears as if the dissociation experiments carried out with permeable resins (24, 32) behave similar to the impermeable dynabeads.

Irreversible binding of labeled DNA to P2 substituted dynabeads was not observed even when 630 nM P2 was used. Thiol activated sepharose resin demonstrated irreversible DNA binding when only 315 nM of P1 was added (24). The irreversible binding of DNA to P1 substituted sepharose resin might be due the presence of many binding sites for DNA due to the high substitution of P1 as proposed by Wren (24). However, comparison of the results obtained by using thiol sepharose resin and dynabeads is not appropriate due to the lack of quantitation of amount of substitution of the labeled DNA to P2 substituted dynabeads.

Dissociation from P2 highly substituted dynabeads

When 315 nM of P2 was used for substitution on dynabeads, the dissociation curve appeared to show a biphasic pattern (Figures 10 and 11). For this data, biphasic

kinetic data analysis was applied (Figures 10C and 11C). There are two rate constants involved in the above dissociation, an initial fast reaction followed by a slow reaction. The reason for this pattern could be due to the presence of more than one binding site with different binding characteristics. However, more data points are required for the slow and fast reaction rates involved when performing biphasic kinetic data analysis. But in the present situation, no more than four data points were taken in the first 30 minutes due to the logistics of the experimental procedure. Thus, the reaction rate calculated for the fast reactions (2×10^{-4} s^{-1} and 8.2×10^{-4} s^{-1}) may not represent the actual reaction rate.

The effect of the concentration of NaCl on the dissociation of P2-DNA complexes

Figure 13 shows that an increase in the concentration of NaCl increased the dissociation of the DNA-P2 complexes. This is in agreement with the results on the effect of concentration of NaCl on the dissociation of DNA-P1 complexes (24). This behavior shows that electrostatic forces play an important in the formation of P2-DNA complexes. Watanabe and Schwarz (20) , Willmitzer and Wagner (21) and Bianchi et al. (18) also concluded from their studies that electrostatic forces play an important role in DNA-protamine interactions.

However, the systems studied by Watanabe and Schwarz, and Willmitzer and Wagner differ significantly from the present system. They studied the interactions between culpeine Z (fish protamine) and large molecular weight DNA. Culpeine Z contains a proline residue which was proposed to cause kinking of the protein. Due to the

large molecular weight DNA, many protamine molecules bind to the same DNA and cooperativity plays an important role in the DNA-protamine and protamine-protamine interactions. Watanabe and Schwarz proposed that the initial contact of culpeine Z with DNA shielded the phosphate groups of the DNA. This would allow other strands of DNA to approach and culpeine Z to bind with the approaching strands of DNA. Thus, the area around culpeine Z would become accessible to higher binding of DNA, leading to positive cooperativity. Willmitzer and Wagner suggested that interactions of Culpeine Z and DNA take place through cross-linking of DNA by Culpeine Z . In the present study, short DNA oligomers and immobilized protamine were used which limits the interaction to small complexes and make cooperativity effects less likely.

Bianchi et al. (18) studied the interaction of DNA fragments of 802, 448, 226, 102 and 48 base pair in length with human protamines P1 and P2 using a gel mobility shift assay. They observed a complete shift in mobility, due to precipitation, for all the lengths of DNA used, at an arginine to phosphate ratio 0.1. Both P1 and P2 behaved similarly in the gel mobility shift assay. The gel mobility shift assay results showed that with or without Zn^{2+}, there was a complete shift at an arginine to phosphate ratio of 0.1. They also studied the effect of concentration of NaCl on DNA - protamine complexes. As the concentration of NaCl was increased from 0.2 M to 0.7 M, the amount of DNA complexed by protamine molecules decreased which indicates that electrostatic interactions predominate. This system also differs from the present system because it involved higher molecular weight DNA molecules compared to the 12 base pair DNA

oligomers used in the present system. In the present system, hamster P2 and bull P1 were used, whereas in the above system, human P1 and P2 were used.

Romaniuk (33) and Record et al. (34) studied the interactions between lysine rich proteins and nucleic acids. Romaniuk plotted a graph between ln K_a and negative ln $[M^+]$ and determined the number of ion pairs formed in the interaction of TF III A and 5S RNA. Record et al. (34) also determined the number of ion pairs formed in the interaction of DNA with polylysine rich protein from the slope of the plot of natural logarithm of equilibrium association constant versus negative ln NaCl concentration. But the present study was different from these studies in many ways. In the two literature studies, the equilibrium binding constants were calculated from which the number of ion pairs involved were calculated. In the present study, only the effect of different concentrations of NaCl on the % cumulative free DNA was determined. So it was not possible to determine the number of ion pairs involved with the data available.

Romaniuk (33) and Record et al. (34) systems involved polylysine rich proteins, whereas the present system involves polyarginine rich proteins. Though both arginine and lysine residues are positively charged, they differ a lot in interactions with other molecules due to the size and resonance of the side chains. Lysine has a simple amine group in its side chain, where as arginine has a complex guanidinium group. Thus, the methods used by Romaniuk (33) and Record et al. (34) to calculate the number ion pairs cannot be applied for the present system.

CONCLUSIONS

The first object of the study was to establish the suitability of tosylactivated dynabeads system as a solid substrate to study DNA-protamine interactions. The use of 0.01% sodium azide in the buffers provided a reduction in nonspecific binding of DNA. Using the tosylactivated dynabeads, it was possible to determine the dissociation rate constant and half lives for the DNA-bull P1 and DNA-hamster P2 complexes. Thus, tosylactivated dynabeads can be used to study the interactions between DNA and protamine molecules, though more work is required to ensure controllable and reproducible substitution of protamine molecules to dynabeads.

The dissociation rate constant of the DNA-bull P1 complexes determined using the dynabead system in two experiments was $3.3 \times 10^{-5} \pm 0.5 \times 10^{-5}$ s^{-1}. This was comparable to the dissociation rate constant of DNA-P1 complexes determined using thiol activated sepharose resin, which was $8.9 \times 10^{-5} \pm 4.4 \times 10^{-5}$ s^{-1} (24).

The dissociation rate constant of the hamster P2-DNA complex determined using the tosylactivated dynabeads in eight experiments was 6.7×10^{-5} $s^{-1} \pm 0.8 \times 10^{-5}$ s^{-1}. An experiment was conducted to determine the dissociation rate constant of P2-DNA complexes using thiol activated sepharose resin as the solid substrate. The k_2 obtained was 3.6×10^{-5} s^{-1}, which is in the same order of magnitude as that obtained using dynabeads. The dissociation rate constants obtained for P2-DNA complexes and P1-DNA complexes are in the same range (10^{-5} s^{-1}).

Bianchi et al. (18) studied the binding characteristics of human P1 and P2 to DNA and concluded that, though the protamines differ structurally, they show functional equivalence in binding DNA. In the present system, when a sufficient amount of DNA was bound to the P1 and P2 substituted dynabeads, it was possible to determine the dissociation rate constant of DNA-protamine complexes. Assuming the dissociation to be a first order reaction, one may compare the dissociation rate constants of bull P1 and hamster P2 with 12 base pair double stranded DNA. The k_2 values obtained for bull P1 and hamster P2 with 12 bp DNA were $3.3 \times 10^{-5} \pm 0.5 \times 10^{-5}$ s^{-1} and 6.7×10^{-5} $s^{-1} \pm 0.8 \times 10^{-5}$ s^{-1} respectively, which are in the same order of magnitude. Thus, the results from this project also suggest functional equivalence of P1 and P2 in binding DNA. However, the limitation of this system appeared to be the lack of reproducible protamine substitution onto the dynabeads.

The increase in the dissociation of the DNA-P2 complexes with an increase in the concentration of NaCl suggests that electrostatic forces play an important role in the formation of DNA-P2 complexes.

REFERENCES

1. Balhorn, R. *In Molecular Biology of Chromosome Function*; Adolph, K. W., Ed.; Springer-Verlag: Newyork, **1989**; Chapter 17.

2. Risley, M. S. *Chromosomes: Eukaryotic, Prokaryotic and Viral*, Kenneth Adolpj, ed., CRC Press, Boca Raton, Florida.

3. Balhorn, R.; Corzett, M.; Mazrimas, J. A. *J. Cell Biol* **1987**, 105, 151a.

4. Gatewood, J. M.; Schroth, G. P.; Schmid, C. W.; Bradbury E. M. *J. Biol. Chem.* **1990**, 265, 20667-20672.

5. Marushige, Y. and Marushige, K. *J. Biol. Chem.* **1975**, 250, 39-45.

6. Weichert, C. K. *Anatomy of the Chordates*; McGraw-Hill: New York, **1951**; pp 357.

7. Louie, A. J.; Dixon, G. H. *J. Biol. Chem.* **1972**, 247, 5498-5505.

8. Candido, E. P. M.; Dixon, G. H. *J. Biol. Chem.* **1972**, 247, 5506-5510.

9. Bode, J.; Willmitzer, L.; Opatz, K. *Eur. J. Biochem.* **1977**, 72, 393-403.

10. Hud, N. V.; Allen, M. J.; Downing, K. H.; Lee, J.; Balhorn, R. *Biochem. Biophys. Res. Commun.* **1993**, 193, 1347-1354.

11. Suau, P.; Subirana, J. A. *J. Mol. Biol.* **1977**, 117, 909-926.

12. Mirzabekov, A. D.; Sanko, D. F.; Kolchinsky, A. M.; Melinkova, A. F. *Eur. J. Biochem.* **1977**, 75, 379-389.

13. Mansy, S.; Engstrom, S. K.; Peticolas, W. L. *Biochem. Biophys. Res. Commun.* **1976**, 68, 1242-1247.

14. Fita, I.; Campos, J. L.; Puigjaner, L. C.; Subiana, J. A. *J. Mol. Biol.* **1982**, 167, 157-177.

15. Warrant, R. W.; Kim, S. H. *Nature* **1978**, 271, 130-135.

16. Balhorn, R. *J. Cell Biol.* **1982**, 93, 298-305.

17. Hud N. V.; Milanovich F. P.; Balhorn R. *J. Biochem.* **1994**, 33, 7528-7535.

18. Bianchi, F.; Prevost, R. R.; Bailly, C.; Rousseaux, J. *Biochem. Biophys. Res. Commun.* **1994**, 201, 1197-1204.

19. Mc Ghee, J.D.; von Hippel, P. H. *J. Mol. Biol.* **1974**, 86, 469-489.

20. Watanabe, F.; Schwarz, G. *J. Mol. Biol.* **1983**, 163, 485-498.

21. Willmitzer, L.; Wagner, K. G. *Biophys. Struct. Mech.* **1980**, 6, 95-110.

22. Yebra D. L.; Ballesca J. L.; Vanrell J. A.; Bassas L.; Oliva R. *J. Biol. Chem.* **1993**, 268, 10553-10557.

23. Gatewood, J. M.; Cook, G. R.; Balhorn, R.; Bradbury, E. M.; Schmid, C. W. *Science* **1987**, 236, 962-964.

24. Wren, J. P.; M.S Thesis, *DNA-Protamine Interactions*, San Jose State University, San Jose, California, **1994**.

25. Jackson, C.J.; Garbett, P.K.; Nissen, B.; Schrieber , L. *J. Cell Science*, **1990**, 96, 257-262.

26. Gladwin, A. M.; Carrier, M. J.; Beesley, J.E.; Lelchuk R.; Hancock, V.; Martin J. F.; *Brit. J. Haema.* **1990**, 76, 333-339.

27. Gabrielsen, O. S.; Huet, J. *In Methods in Enzymology*, Academic Press: New York, **1993**, 36, 508-526.

28. Hultman, T.; Stahl, S.; Hornes, E.; Uhlen, M. *Nucleic Acids Res.* **1989**, 17, 4937-4946.

29. Lillehaug, J. R.; Kleppe, R. K.; Kleppe, K. *Biochemistry*, **1976**, 15, 1858-1865.

30. Young H. D. *Statistical Treatment of Experimental Data*, McGraw-Hill: New York, **1962**.

31. Moore, J. W.; Pearson, R. G. *Kinetics and Mechanism*, 3rd ed; John Wiley & Sons:

New York, **1981**, Chapter 3.

32. Poenisch, P.; M.S Thesis, *Dissociation Rate Constant Measurement for Double Stranded DNA-Protamine P1*, San Jose State University, San Jose, California, **1996**.

33. Romaniuk, P. J. *Nucleic Acids Res.*, **1985**, 13, 5369-5387

34. Record, M. T., Jr.; Lohman, T. M.; de Haseth, P. *J. Mol. Biol.* **1976**, 107, 145-158.

4/10/97

From

Syamala Akkaraju
Graduate Student, Chemistry Department
San Jose State University
One Washington Square
San Jose, CA, 95192-0025

To

Dr. Gatewood
Mail Stop M880, Life sciences Division
Los Alamos National Laboratory
Los Alamos, NM 87545

Dear Dr. Gatewood,

I am a graduate student at San Jose State University, San Jose, California, finishing my M. S. in Chemistry. I would like to include in my thesis, a figure (Figure no. 9, page no. 20671) from the journal of Biological Chemistry (1990), Vol. 256, "Zinc-induced Secondary Structure Transtitions in Human Sperm Protamines", authored by you, Gary P. Schroth, Carl W . Schmid, and E. Morton Bradbury. Three copies of my thesis will be published. The title of my thesis is "DNA-Protamine interactions", presented to the faculty of the department of Chemistry, San Jose State University.

I would like to receive written permission from you in this regard. I can be reached by fax, care of Dr. Stacks at (408) 924-4945.

Thank You

Yours truly

S. Syamala.

Syamala Akkaraju

4/10/97

From

Syamala Akkaraju
Graduate Student, Chemistry Department
San Jose State University
One Washington Square
San Jose, CA, 95192-0025

To

McGraw-Hill Book Company, Inc.
1221 Avenue of the Americas
New York, NY 10020

Dear Sir,

I am a graduate student at San Jose State University, San Jose, California, finishing my M. S. in Chemistry. I would like to include in my thesis, a figure (Figure no.8.27, page no. 357) from the book "Anatomy of the Chordates", First edition (1951), authored by Charles K. Weichert. Three copies of my thesis will be published. The title of my thesis is "DNA-Protamine interactions", presented to the faculty of the department of Chemistry, San Jose State University.

I would like to receive written permission from you in this regard. I can be reached by fax, care of Dr. Stacks at (408) 924-4945.

Thank You

Yours truly

S. Syamala.

Syamala Akkaraju